Accepted Manuscript

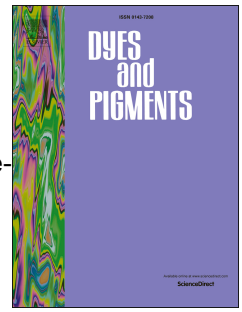

Synthesis and photophysical properties of fluorescent arylstyrylimidazo[1,2-a]pyridine-based donor-acceptor chromophores

Zeynel Seferoğlu, Heiko Ihmels, Ertan Şahin

PII: S0143-7208(14)00375-1

DOI: 10.1016/j.dyepig.2014.09.016

Reference: DYPI 4529

To appear in: *Dyes and Pigments*

Received Date: 23 July 2014

Revised Date: 1 September 2014

Accepted Date: 9 September 2014

Please cite this article as: Seferoğlu Z, Ihmels H, Şahin E, Synthesis and photophysical properties of fluorescent arylstyrylimidazo[1,2-a]pyridine-based donor-acceptor chromophores, *Dyes and Pigments* (2014), doi: 10.1016/j.dyepig.2014.09.016.

Graphical Abstract (for review)

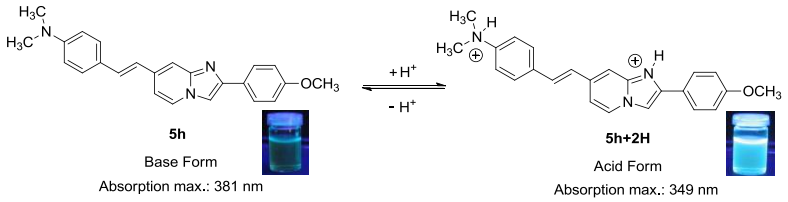

Highlights

- A series of novel fluorescent arylstyrylimidazo[1,2-a]pyridine-based dyes was efficiently synthesized and characterized.
- The arylstyrylimidazo[1,2-a]pyridine dyes exhibit fluorosolvatochromism.
- These compounds may be used as pH-sensitive fluorescent light-up probe because they display strong changes of absorption and emission properties with decreasing pH.

Synthesis and photophysical properties of fluorescent arylstyrylimidazo[1,2-a]pyridine-based donor-acceptor chromophores

Zeynel Seferoğlu[a,b] *, Heiko Ihmels[b] and Ertan Şahin[c]

[a]*Gazi University, Department of Chemistry, 06500 Ankara, Turkey*

[b]*University of Siegen, Organic Chemistry II, Adolf-Reichwein-Str. 2, D-57068 Siegen, Germany*

[c]*Atatürk University, Department of Chemistry, Erzurum, Turkey*

Abstract

A series of novel fluorescent arylstyrylimidazo[1,2-a]pyridines was synthesized and fully characterized. All styryl derivatives have an *E*-configuration of the vinyl double bond as unequivocally shown by ^{1}H NMR spectroscopy. It was observed that the *E* isomers are stable in the solid state; however, the derivatives with strong electron donating dialkylamino substituents underwent partial *E-Z* isomerization in solution at room temperature. The styryl derivatives absorb in the UV or visible region and emit light with moderate Stokes shifts. These compounds exhibit fluorosolvatochromism, namely the emission band is red shifted with increasing solvent polarity. Moreover, the absorption and emission properties of the styryl derivatives change drastically upon acidification, as the protonation of the nitrogen atoms of the imidazo[1,2-a]pyridine ring increases the donor-acceptor interplay of the π system.

Keywords: Styryl dyes, heterocycles, imidazo[1,2-a]pyridine, pH sensitive dyes, fluorescent probes.

*Corresponding author Tel.: +90 312 2021525; fax: +90 312 2122279

**E-mail addresses*: znseferoglu@gazi.edu.tr (Z. Seferoğlu).

1. Introduction

Functional dyes with appropriate absorption and emission color are useful components for the development of optical chemosensors, photonic materials or photosensitizers [1-4]. Specifically, fluorescent chemosensors are versatile tolls in analytical chemistry, biochemistry and medicine [5]. These probe molecules may be employed for the fluorimetric characterization of their surounding environment, because the latter may affect the emission energy, emission quantum yield, or emission lifetime [6,7]. Along these lines, styryl dyes have been established as a promising class of compounds that exhibit a great potential to be employed in advanced materials such as laser dyes, optical or electro-optical devices or sensor materials [8-31] etc. due to their excellent optical-electronic properties. Also, many potential metal-free solar cell sensitizers are neutral styryl dyes [32]. However, some neutral styryl dyes also show thermally induced or photo-induced *E-Z* isomerization and dimerization especially in solution [33]. In addition, the cationic styryl dyes are used as DNA probes and voltage-sensitive dyes in cardiac tissue [34-37]. Overall, the class of styryl dyes exhibits a remarkable structural diversity. And among the substructures that are frequently used for the development of functional styryl dyes, nitrogen-containing heterocyles constitute a highly variable and versatile component [26]. In this context it is surprising that imidazopyridine rings have not been explored systematically as heteroaromatic unit in styryl dyes. Imidazopyridine rings systems are well-known heterocyclic compounds with a large potential to exhibit biological activity [38-43]. In addition these heterocycles are readily available and functionalized. Therefore we proposed that the integration of imidazopyridine units into styryl-type structures leads to novel dye structures with promising properties that may be considered for the development of functional dyes. Herein we present the synthesis and and investigation of photophysical properties of arylstyrylimidazo[1,2-a]pyridine dyes.

2. Experimental Section

2.1. General Instrumentations and Materials

All commercially available chemicals were reagent grade and used without further purification. The melting points were determined with a Büchi 510K melting point apparatus and are not corrected. Mass spectra (ESI in the positive-ion mode, source voltage 6 kV) were recorded with a Finnigan LCQ Deca instrument; only *m/z* values in the range of 100-2000 units were analyzed. NMR spectra were measured on Bruker Avance 400 (^{1}H: 400 MHz, ^{13}C: 100 MHz) spectrometers at 20 °C (293 K); chemical shifts are given in ppm (δ) relative to TMS (δ = 0.00 ppm). Elemental microanalysis of the compounds was performed with a HEKAtech EuroEA combustion analyzer by Mr. H. Bodenstedt (Organische Chemie I, Universität Siegen). The X-ray diffraction data collection was performed on a Rigaku R-AXIS RAPID-S diffractometer equipped with Mo Kα (λ=0.71073 Å) radiation using w scans.

2.2. Spectrophotometric measurements.

Absorption spectra were recorded on a Varian Cary 100 double-beam spectrophotometer; steady-state fluorescence spectra were recorded on a Varian Cary Eclipse fluorescence spectrophotometer. All spectrophotometric measurements were performed in thermostated quartz sample cells at 20 °C, using spectral grade solvents (Fluka, Riedel-de Haën). The solution concentrations were 10 μM for absorption spectroscopy and 1.0-5.0 μM for fluorescence spectroscopy. Spectrophotometer slit widths were set to bandwidths of 5 nm for emission spectroscopy. The relative fluorescence quantum yields, Φ_{fl}, were determined by

standard methods [44,45] with Coumarin 1 (laser grade, Acros Organics, Φ_{fl} = 0.73 in ethanol) as a reference.

2.3. X-ray crystallography

Single crystal X-ray diffraction data were collected on Rigaku R-AXIS RAPID-S diffractometer equipped with a IP detector, using monochromatized Mo K_α (λ=0.71073 A°) radiation. Integration of the intensities, correction for Lorentz and polarization effects and cell refinements were performed using CrystalClear (Rigaku/MSC Inc., 2005) software [46]. The structures were solved by direct methods SHELXS97 [47] and refined on F^2 by full-matrix least-squares using the programs SHELXL97 [47]. All non-hydrogen atoms were refined anisotropically. Positions of H atoms bonded to C atoms were calculated at ideal positions and refined by the riding model with Uiso -1.5U_{eq}(C) for methyl, and Uiso -1.2Ueq(C) for remaining H atoms. The final difference Fourier maps showed no peaks of chemical significance. Crystal data and details of the structure determination for the compounds are summarized in Table S1 (in Supporting information page S5).

2.4. General procedure for the synthesis of imidazo[1,2-a]pyridine derivatives 3a-c.

A mixture of respective 2-bromoacetophenone derivative (0.001 mol) the 2-amino-4-methylpyridine (0.001 mol, 0.108 g) and $NaHCO_3$ (0.84 g, 0.01 mol) in EtOH (95%, 20 mL) was stirred under reflux for 20 h. The reaction progress was monitored by TLC. Upon completion of the reaction, the mixture was evaporated to dryness and the residue was dissolved in $CHCl_3$ and dried with $MgSO_4$. The solvent was evaporated under reduced

pressure. The precipitate was filtered and dried. The crude product was recrystallized from ethanol to yield the pure compound as crystal. Characterization data for compounds is presented here.

2-phenyl-7-methylimidazo[1,2-a]pyridine (3a). Light colorless crystals were obtained after recrystalization by ethanol in 73% yield (0.15 g); mp. 167-168 ℃ (lit. mp: 165-167 ℃ [48]); ^{1}H NMR ($CDCl_3$): δ 2.38 (s, 3H), 6.59 (dd, 1H), 7.31-7.33 (m, 1H), 7.40-7.44 (m, 3H), 7.76 (s, 1H), 7.92-7.98 (m, 3H); MS (ESI^+): *m/z* = 209.5 $[M+H]^+$; Anal. Calcd for $C_{14}H_{12}N_2$: C, 80.74; H, 5.81; N, 13.45. Found: C, 80.88; H, 6.04; N, 13.34.

2-(4-Methoxyphenyl)-7-methylimidazo[1,2-a]pyridine (3b). Light yellow crystals were obtained after recrystalization by ethanol in 82% yield (0.20 g); mp. 163-165 ℃ ((lit. mp: 164-165 ℃ [49]); ^{1}H NMR ($CDCl_3$): δ 2.39 (s, 3H), 3.82 (s, 3H), 6.58 (dd, 1H), 6.94-6.97 (d, 2H, *J* = 8.8 Hz), 7.38 (br s, 1H), 7.68 (s, 1H), 7.85-7.87 (d, 2H, *J* = 8.8 Hz), 7.96 (d, 1H); MS (ESI^+): *m/z* = 239 $[M+H]^+$; Anal. Calcd for $C_{15}H_{14}N_2O$: C, 75.61; H, 5.92; N, 11.76. Found: C, 75.76; H, 5.89; N, 11.83.

2-(4-Bromophenyl)-7-methylimidazo[1,2-a]pyridine (3c). Light colorless crystals were obtained after recrystalization by ethanol in 79% yield (0.23 g); mp. 219-220 ℃ ((lit. mp. 216-217 ℃ [50]); ^{1}H NMR ($CDCl_3$): δ 2.39 (s, 3H), 6.59 (dd, 1H), 7.36 (br s, 1H), 7.51-7.54 (d, 2H, *J* = 8.6 Hz), 7.73 (s, 1H), 7.73-7.94 (d, 2H, *J* = 8.6 Hz), 7.96 (d, 1H); MS (ESI^+): *m/z* = 289.6 $[M+H, {}^{81}Br]^+$; Anal. Calcd for $C_{14}H_{11}N_2Br$: C, 58.56; H, 3.86; N, 9.76. Found: C, 58.42; H, 3.82; N, 9.61.

2.5. General procedure for the synthesis of the imine derivatives 4a-f.

Equimolar mixture of various substituted aldehyde (10 mmol) and 4-chloroaniline (10 mmol) in methanol (15 ml) was refluxed for 4 h. After cooling, filtration and drying. The crude product was recrystallized from methanol or ethanol to yield the pure compound as powder or crystal.

N-Benzylidene-4-chloroaniline (4a): Light yellow crystals were obtained after recrystalization from ethanol; 74% yield (1.60 g); mp. 63-64 °C (lit. mp. 53-56 °C [51]); ^{1}H NMR ($CDCl_3$): δ 7.14-7.16 (d, 2H, J = 8.8 Hz), 7.34-7.36 (d, 2H, J = 8.8 Hz), 7.47-7.49 (d, 2H, J = 8.6 Hz), 7.88-7.90 (d, 2H, J = 8.6 Hz), 8.43 (s, 1H).

4-Chloro-N-[4-(piperidinylamino)benzylidene]aniline (4b): Yellow crystals were obtained after recrystalization from ethanol; yield 86% (2.56 g); m.p. 136-137 °C (lit. mp. 135-137 °C [52]); ^{1}H NMR ($CDCl_3$): δ 1.66-1.69 (m, 6H), 3.32-3.34 (m, 4H), 6.91-6.93 (d, 2H, J = 8.6 Hz), 7.11-7.13 (d, 2H, J = 9.1 Hz), 7.30-7.32 (d, 2H, J = 9.1 Hz), 7.74-7.76 (d, 2H, J = 8.6 Hz), 8.43 (s, 1H).

4-Chloro-N-[4-(diethylamino)benzylidene]aniline (4c): Light yellow crystals were obtained after recrystalization from ethanol; yield 89% (2.55 g); mp. 93-94 °C, (lit. mp. 94-95 °C [53]); ^{1}H NMR ($CDCl_3$): δ 1.18-1.22 (t, 4H), 3.39-3.44 (q, 6H), 6.67-6.70 (d, 2H, J = 9.1 Hz), 7.10-7.13 (d, 2H, J = 9.1 Hz), 7.29-7.31 (d, 2H, J = 9.1 Hz), 7.72-7.74 (d, 2H, J = 9.1 Hz), 8.24 (s, 1H).

4-Chloro-N-[4-(dimethylamino)benzylidene]aniline (4d): Yellow powder were obtained after recrystalization from methanol; yield 82% (2.12 g); mp. 156-157 °C (lit. mp. 135-137 °C [52]); ^{1}H NMR ($CDCl_3$): δ 3.12 (s, 6H), 6.71-6.73 (d, 2H, *J* = 8.7 Hz), 7.12-7.14 (d, 2H, *J* = 8.7 Hz), 7.30-7.32 (d, 2H, *J* = 8.5 Hz), 7.76-7.78 (d, 2H, *J* = 8.6 Hz), 8.28 (s, 1H).

4-Chloro-N-[4-methylsulfanylbenzylidene]aniline (4e): Yellow powder were obtained after recrystalization from ethanol; yield 88% (2.30 g); mp. 126-127 °C; ^{1}H NMR ($CDCl_3$): δ 2.52 (s, 3H, SCH_3), 7.13-7.15 (d, 2H, *J* = 8.7 Hz), 7.28-7.30 (d, 2H, *J* = 8.4 Hz), 7.32-7.34 (d, 2H, *J* = 8.5 Hz), 7.78-7.80 (d, 2H, *J* = 8.6 Hz), 8.36 (s, 1H).

4-Chloro-N-[4-methoxybenzylidene]aniline (4f): White crystals were obtained after recrystalization from methanol; yield 85% (1.98 g); mp: 101-102 °C (lit. mp: 90-94 °C [52]); ^{1}H NMR ($CDCl_3$): δ 3.89 (s, 3H, OCH_3), 6.97-6.98 (d, 2H, *J* = 8.8 Hz), 7.16-7.18 (d, 2H, *J* = 8.7 Hz), 7.33-7.35 (d, 2H, *J* = 8.7 Hz), 7.87-7.89 (d, 2H, *J* = 8.8 Hz), 8.36 (s, 1H).

4-Chloro-N-thiophene2-ylbenzylideneaniline (4g): Light brown powder were obtained after recrystalization from ethanol; yield 81% (1.79 g); mp: 74-75 °C; ^{1}H NMR ($CDCl_3$): δ 7.10-7.33 (d, 2H, *J* = 8.8 Hz), 7.48-7.61 (d, 2H, *J* = 8.7 Hz), 7.57 (m, 1H), 7.73 (m, 1H), 7.92 (d, 1H), 8.33 (s, 1H).

2.6. General procedure for the synthesis of styrylimidazo[1,2-a]pyridine derivatives.

A stirred mixture of various 2-substituted-7-methylimidazo[1,2-a]pyridine (0.01 mol) and K^{t}BuO (0.25 mol) and the corresponding imine derivatives (0.01 mol) in DMF (20 mL) was

heated at 90 °C for 4 h. The mixture was allowed to cool and methanol/water mixture (10:1) was added. The precipitate was filtered and dried. The crude product was recrystallized from EtOAc or EtOAc/MeOH to yield the pure compound as crystalline solid or as fine powder.

7-[(*E*)-2-(phenyl)vinyl]-2-phenylimidazo[1,2-a]pyridine (5a): The formed solid was collected by filtration and recrystallized from EtOAc/DME to give compound as light brown solid in 74% yield (2.19 g); mp: 211-212 °C (lit. mp 207-208 °C [54]); ^{1}H NMR ($CDCl_3$) δ 7.10-7.14 (m, 2H), 7.17-7.21 (d, 1H, J_{trans} = 16.0 Hz), 7.31-7.49 (m, 6H), 7.56-7.58 (d, 1H), 7.68 (s br 1H), 7.85 (s, 1H), 7.98-8.0 (d, 2H), 8.0-8.1 (d, 1H); ^{13}C NMR (100 MHz, $CDCl_3$): δ 109.2, 111.1, 115.9, 113.1, 116.4, 126.1, 126.9, 127.6, 128.9, 129.1, 129.6, 129.7, 131.4, 137.5, 144.5, 146.4, 159.6; MS (ESI^+): *m/z* = 297.8 $[M]^+$; Anal. Calcd for $C_{21}H_{16}N_2$: C, 85.11; H, 5.44; N, 9.45 Found: C, 85.01; H, 5.21; N, 9.28.

7-[(*E*)-2-(phenyl)vinyl]-2-(4-methoxyphenyl)imidazo[1,2-a]pyridine (5b): The formed solid was collected by filtration and recrystallized from EtOAc to give compound as light yellow crystals in 82% yield (2.67 g); mp: 239-240 °C (lit. mp 232-233 °C [54]); ^{1}H NMR ($CDCl_3$) δ 3.83 (s, 3H), 6.99-7.02 (d, 2H, *J* = 8.8 Hz), 7.07-7.09 (dd, 1H), 7.09-7.14 (d, 1H, J_{trans} = 16.3 Hz), 7.15-7.19 (d, 1H, J_{trans} = 16.3 Hz), 7.30-7.34 (m, 1H), 7.39-7.42 (m, 2H), 7.56-7.58 (d, 2H, *J* = 8.6 Hz), 7.62 (s br 1H), 7.71 (s, 1H), 7.90-7.92 (d, 2H, *J* = 8.8 Hz), 8.06-8.08 (d, 1H); ^{13}C NMR (100 MHz, $CDCl_3$): δ 56.1, 108.3, 110.9, 115.0, 115.7, 121.2, 125.9, 127.5, 127.6, 128.1, 129.0, 131.2, 133.4, 134.8, 137.4, 142.8, 144.5, 160.5; MS (ESI^+): *m/z* = 327.8 $[M]^+$; Anal. Calcd for $C_{22}H_{18}N_2O$: C, 80.96; H, 5.56; N, 8.58. Found: C, 80.89; H, 5.53; N, 8.44.

7-[(*E*)-2-(4-Piperidinylaminophenyl)vinyl]-2-phenylimidazo[1,2-a]pyridine (5c): The formed solid was collected by filtration and recrystallized from EtOAc/MeOH to give compound as yellow powder in 88% yield (3.34 g); mp: 293-294 °C; ^{1}H NMR ($CDCl_3$) δ 1.61-1.62 (m, 2H), 1.70-1.72 (m, 4H), 3.23-3.26 (m, 4H), 6.91-6.94 (m, 3H), 7.10-7.14 (m, 2H), 7.35-7.36 (m, 1H), 7.42-7.47 (m, 4H), 7.68 (s, 1H), 7.79 (s, 1H), 7.96-7.98 (d, 2H, J = 9.1 Hz), 8.05-8.06 (d, 1H); ^{13}C NMR (100 MHz, $CDCl_3$): δ 24.6, 25.4, 49.1, 108.0, 115.6, 124,1, 125.4, 126.2, 128.2, 128.9, 131.9, 134.0, 138,4, 144.6, 146.6, 148.3, 156.1, 159.4, 160.6; MS (ESI$^+$): *m/z* = 380.8 $[M]^+$, 759.6, 760.6 (Dimer); Anal. Calcd for $C_{26}H_{25}N_3$: C, 82.29; H, 6.64; N, 11.07 Found: C, 82.11; H, 6.52; N, 11.01.

7-[(*E*)-2-(4-Piperidinylaminophenyl)vinyl]-2-(4-methoxyphenyl)imidazo[1,2-a]pyridine (5d): The formed solid was collected by filtration and recrystallized from EtOAc/MeOH to give compound as brillant yellow powder in 88% yield (3.40 g); mp: 292-293 °C; ^{1}H NMR ($CDCl_3$) δ 1.60-1.63 (m, 2H), 1.69-1.72 (m, 4H), 3.24-3.27 (m, 4H), 3.84 (s, 3H, OCH_3), 6.88-6.92 (m, 3H), 6.96-6.98 (d, 2H, J = 8.8 Hz), 7.11-7.15 (m, 2H), 7.41-7.43 (d, 2H, J = 8.8 Hz), 7.70 (s, 1H), 7.72 (s, 1H), 7.89-7.92 (d, 2H, J = 8.7 Hz), 8.05-8.07 (d, 1H); ^{13}C NMR (100 MHz, $CDCl_3$): δ 24.7, 25.9, 50.5, 54.9, 107.5, 115.3, 112.5, 114.8, 116.6, 122.4, 125.7, 126.7, 127.1, 128.0, 128.5, 132.6, 144.5, 145.6, 155.4, 160.1; MS (ESI$^+$): *m/z* = 410.7 $[M]^+$, 819.1, 820.1 (Dimer) Anal. Calcd for $C_{27}H_{27}N_3O$: C, 79.19; H, 6.65; N, 10.26 Found: C, 78.96; H, 6.59; N, 10.11.

7-[(*E*)-2-(4-Diethylaminophenyl)vinyl]-2-phenylimidazo[1,2-a]pyridine (5e): The formed solid was collected by filtration and recrystallized from EtOAc/MeOH to give compound as dark yellow crystals in 84% yield (3.08 g); mp: 174-175 °C; ^{1}H NMR ($CDCl_3$) δ 1.15-1.20 (t, 4H), 3.36-3.41 (q, 6H), 6.65-6.67 (d, 2H, J = 8.8Hz), 6.84-6.88 (d, 1H, J_{trans} = 16.1 Hz), 7.02-

7.08 (m, 2H), 7.32-7.34 (m, 1H), 7.39-7.45 (m, 4H), 7.54 (s, 1H), 7.77 (s, 1H), 7.94-7.96 (d, 2H, J = 8.4 Hz), 7.98-8.0 (d, 1H); ^{13}C NMR (100 MHz, $CDCl_3$): δ 12.6, 44.4, 108.0, 110.4, 111.6, 113.3, 121.4, 123.7, 125.0, 125.9, 128.0, 128.2, 128.3, 128.7, 130.4, 131.1, 133.3, 136.0, 146.1, 147.8; MS (ESI^+): m/z = 368.6 $[M]^+$, 735.1, 736.2 (Dimer); Anal. Calcd for $C_{25}H_{25}N_3$: C, 81.71; H, 6.86; N, 11.43 Found: C, 81.86; H, 6.84; N, 11.43.

7-[(*E*)-2-(4-Diethylaminophenyl)vinyl]-2-(4-methoxyphenyl)imidazo[1,2a]pyridine (5f): The formed solid was collected by filtration and recrystallized from EtOAc/MeOH to give compound as yellow powder in 83% yield (3.30 g); mp: 230-231 °C; ^{1}H NMR ($CDCl_3$) δ 1.17-1.20 (t, 4H), 3.36-3.41 (q, 6H), 3.85 (s, OCH_3), 6.65-6.68 (d, 2H, J = 8.8 Hz), 6.84-6.88 (d, 1H, J_{trans} = 16.1 Hz), 6.95-6.98 (d, 2H, J = 8.7 Hz), 7.0-7.20 (m, 1H), 7.02-7.07 (d, 1H, J_{trans} = 16.1 Hz), 7.39-7.41 (d, 2H, J = 8.6 Hz), 7.49 (s, 1H), 7.69 (s, 1H), 7.86-7.89 (d, 2H, J = 8.8 Hz), 7.97-7.99 (d, 1H); ^{13}C NMR (100 MHz, $CDCl_3$): δ 12.6, 44.4, 55.3, 107.1, 109.9, 111.6, 113.6, 114.1, 121.7, 123.8, 124.8, 126.6, 127.2, 128.1, 130.5, 135.3, 146.1, 147.7, 159.5; MS (ESI^+): m/z = 398.6 $[M]^+$, 795.2, 796.2 (Dimer); Anal. Calcd for $C_{26}H_{27}N_3O$: C, 78.56; H, 6.85; N, 10.57 Found: C, 78.44; H, 6.75; N, 10.55.

7-[(*E*)-2-(4-Dimethylaminophenyl)vinyl]-2-phenylimidazo[1,2-a]pyridine (5g): The formed solid was collected by filtration and recrystallized from EtOAc/MeOH to give compound as yellow needle crystals in 84% yield (2.85 g); mp: 291-292 °C; ^{1}H NMR ($CDCl_3$) δ 3.0 (s, 6H), 6.69-6.73 (d, 2H, J = 8.8 Hz), 6.86-6.91 (d, 1H, J_{trans} = 16.2 Hz), 7.10-7.14 (m, 2H), 7.30-7.32 (m, 1H), 7.41-7.68 (m, 4H), 7.68 (s br 1H), 7.78 (s, 1H), 7.96-7.98 (d, 2H, J = 8.5 Hz), 8.04-8.06 (d, 1H); ^{13}C NMR (100 MHz, $CDCl_3$): δ 40.3, 108.4, 112.6, 112.6, 121.9, 125.5, 126.1, 128.2, 128.5, 128.9, 130.5, 131.8, 135.3, 145.9, 147.8; MS (ESI^+): m/z =

340.6 $[M]^+$, 679.1, 680.2 (Dimer); Anal. Calcd for $C_{23}H_{21}N_3$: C, 81.38; H, 6.24; N, 12.38 Found: C, 81.19; H, 6.25; N, 12.39.

7-[(*E*)-2-(4-Dimethylaminophenyl)vinyl]-2-(4-methoxyphenyl)imidazo[1,2a]pyridine (5h): The formed solid was collected by filtration and recrystallized from EtOAc/MeOH to give compound as light yellow needle crystals in 88% yield (3.25 g); mp: 280-281 °C; ^{1}H NMR ($CDCl_3$) δ 3.0 (s, 6H), 3.85 (s, 3H) 6.70-6.72 (d, 2H, J = 8.8 Hz), 6.86-6.90 (d, 1H, J_{trans} = 16.2 Hz), 6.96-6.98 (d, 2H, J = 8.8 Hz), 7.06-7.12 (m, 2H), 7.42-7.44 (d, 2H, J = 8.8 Hz), 7.61 (s br 1H), 7.69 (s, 1H), 7.88-7.90 (d, 2H, J = 8.8 Hz), 8.01-8.02 (d, 1H); ^{13}C NMR (100 MHz, $CDCl_3$): δ 40.5, 55.8, 107.2, 110.5, 112.3, 114.6, 121.9, 124.7, 125.0, 127.3, 128.0, 130.6, 135.8, 144.8, 145.0, 146.2, 150.5, 160.8; MS (ESI^+): m/z = 370.9 $[M]^+$, 739.6 (Dimer); Anal. Calcd for $C_{24}H_{23}N_3O$: C, 78.02; H, 6.27; N, 11.37 Found: C, 77.83; H, 6.18; N, 11.21.

7-[(*E*)-2-(4-Methylsulfanylphenyl)vinyl]-2-phenylimidazo[1,2-a]pyridine (5i): The formed solid was collected by filtration and recrystallized from EtOAc/MeOH to give compound as light yellow powder in 79% yield (2.70 g); mp: 250-251 °C; ^{1}H NMR ($CDCl_3$) δ 2.56 (s, 3H, SCH_3), 7.03-7.06 (d, 1H, J_{trans} = 16.0 Hz), 7.09-7.13 (d, 1H, J_{trans} = 16.1 Hz), 7.23-7.26 (d, 2H, J = 8.4 Hz), 7.32-7.36 (m, 1H), 7.42-7.47 (m, 4H), 7.63 (s br 1H), 7.82 (s, 1H), 7.94-7.97 (d, 2H, J = 8.6 Hz), 8.05-8.07 (d, 1H); ^{13}C NMR (100 MHz, $CDCl_3$): δ 16.4, 109.1, 111.0, 115.8, 126.0, 126.8, 127.4, 127.9, 128.9, 129.5, 130.5, 134.2, 139.6 (The some signals are not observed); MS (ESI^+): m/z = 343.5 $[M+H]^+$, 685.0 (Dimer); Anal. Calcd for $C_{22}H_{18}N_2S$: C, 77.16; H, 5.30; N, 8.18, S, 9.36 Found: C, 77.03; H, 5.22; N, 8.11, S, 9.33.

7-[(*E*)-2-(4-Methylsulfanylphenyl)vinyl]-2-(4-methoxyphenyl)imidazo[1,2a]pyridine (5j): The formed solid was collected by filtration and recrystallized from EtOAc/MeOH to give

compound as light yellow powder in 77% yield (2.87 g); mp: 268-269 °C; ^{1}H NMR ($CDCl_3$) δ 2.53 (s, 3H, SCH_3), 3.87 (s, 3H, OCH_3), 6.98-7.0 (d, 2H, J = 8.8 Hz), 7.03-7.07 (d, 1H, J_{trans} = 16.3 Hz), 7.16-7.20 (d, 1H, J_{trans} = 16.3 Hz), 7.24-7.27 (d, 2H), 7.45-7.47 (d, 2H, J = 8.4 Hz), 7.73 (s br 1H), 7.86 (s, 1H), 7.92-7.94 (d, 2H, J = 8.7 Hz), 8.10-8.12 (d, 1H); ^{13}C NMR (100 MHz, $CDCl_3$): It was not obtained good spectrum; MS (ESI^+): m/z = 373.8 $[M+H]^+$, 745.2 (Dimer); Anal. Calcd for $C_{22}H_{18}N_2S$: C, 74.16; H, 5.41; N, 7.52, S, 8.61 Found: C, 73.97; H, 5.38; N, 7.44, S, 8.55.

7-[(*E*)-2-(4-Methoxyphenyl)vinyl]-2-phenylimidazo[1,2-a]pyridine (5k): The formed solid was collected by filtration and recrystallized from EtOAc/MeOH to give compound as light yellow powder in 75% yield (2.70 g); mp: 261−263 °C (lit. mp. 243-244 °C [54]); ^{1}H NMR ($CDCl_3$) δ 3.04 (s, 3H, OCH_3), 6.91-6.93 (d, 2H, J = 8.8 Hz), 6.95-6.99 (d, 1H, J_{trans} = 16.4 Hz), 7.04-7.06 (dd, 1H), 7.08-7.12 (d, 1H, J_{trans} = 16.3 Hz), 7.33-7.35 (m, 1H), 7.42-7.49 (m, 4H), 7.57 (s br 1H), 7.82 (s, 1H), 7.94-7.97 (d, 2H, J = 8.7 Hz), 8.04-8.05 (d, 1H); ^{13}C NMR (100 MHz, $CDCl_3$): δ 55.4, 108.2, 111.5, 114.6, 115.5, 120.6, 124.7, 125.2, 126.8, 128.2, 128.9, 129.4, 132.4, 134.3, 136.4, 144.2, 145.8, 159.8; MS (ESI^+): *m/z* = 327.4 $[M+H]^+$, 652.9 (Dimer); Anal. Calcd for $C_{22}H_{18}N_2O$: C, 80.96; H, 5.56; N, 8.58 Found: C, 81.03; H, 5.35; N, 8.43.

7-[(*E*)-2-(4-Methoxyphenyl)vinyl]-2-(4-methoxyphenyl)imidazo[1,2a]pyridine (5l):

The formed solid was collected by filtration and recrystallized from EtOAc to give compound as pale yellow powder in 78% yield (2.78 g); mp: 275-276 °C (lit. mp. 266-267 °C [54]); ^{1}H NMR ($CDCl_3$) δ 3.84 (s, 3H, OCH_3), 3.86 (s, 3H, OCH_3), 6.91-6.93 (d, 2H, J = 8.7 Hz), 6.95-6.99 (d, 1H, J_{trans} = 16.3 Hz), 6.91-7.0 (d, 2H, J = 8.9 Hz), 7.06-7.08 (dd, 1H), 7.10-7.14 (d, 1H, J_{trans} = 16.3 Hz), 7.47-7.50 (d, 2H, J = 8.7 Hz), 7.62 (s br 1H), 7.73 (s, 1H), 7.89-7.91 (d,

2H, *J* = 8.8 Hz), 8.04-8.05 (d, 1H); ^{13}C NMR (100 MHz, $CDCl_3$): δ 55.2, 55.9, 109.1, 111.4, 113.2, 114.9, 121.8, 125.9, 127.3, 128.8, 129.3, 130.6, 131.7, 144.8, 145.1, 159.8, 161.6 (The some signals are not observed); MS (ESI^+): *m/z* = 357.7 $[M+H]^+$, 713.3 (Dimer); Anal. Calcd for $C_{23}H_{20}N_2O_2$: C, 77.51; H, 5.66; N, 7.86 Found: C, 77.28; H, 5.58; N, 7.71.

7-[(*E*)-2-thienylvinyl]-2-(4-methoxyphenyl)imidazo[1,2a]pyridine (5m): The formed solid was collected by filtration and recrystallized from EtOAc/MeOH to give compound as pale yellow powder in 88% yield (2.78 g); mp: 227-228 °C (lit. mp: 222-223 °C [54]); ^{1}H NMR ($CDCl_3$) *δ* 3.85 (s, 3H, OCH_3), 6.87-6.91 (d, 1H, J_{trans} = 16.0 Hz), 6.96-6.98 (d, 2H, *J* = 8.8 Hz), 6.98-6.99 (dd, 1H), 7.02-7.04 (m, 2H), 7.12-7.13 (d, 1H), 7.24-7.28 (d, 1H, J_{trans} = 16.3 Hz), 7.57 (s br 1H), 7.73 (s, 1H), 7.87-7.89 (d, 2H, *J* = 8.8 Hz), 8.02-8.05 (d, 1H); ^{13}C NMR (100 MHz, $CDCl_3$): δ 55.3, 107.5, 110.1, 114.2, 114.3, 123.6, 125.1, 125.3, 126.1, 127.1, 127.3, 127.8, 133.1, 137.0, 142.1, 144.5, 145.6, 159.7; MS (ESI^+): *m/z* = 333.7 $[M+H]^+$, 665.1 (Dimer); Anal. Calcd for $C_{20}H_{16}N_2OS$: C, 72.26; H, 4.85; N, 8.43; S, 9.65 Found: C, 72.11; H, 4.79; N, 8.33; S, 9.48.

7-[(*E*)-2-thienylvinyl]-2-(4-bromophenyl)imidazo[1,2a]pyridine (5n): The formed solid was collected by filtration and recrystallized from EtOAc/MeOH to give compound as yellow powder in 83% yield (3.16 g); mp: 255-256 °C; ^{1}H NMR ($CDCl_3$) δ 6.87-6.91 (d, 1H, J_{trans} = 16.1 Hz), 7.02-7.05 (m, 2H), 7.13-7.14 (d, 1H), 7.27-7.30 (d, 1H, J_{trans} = 16.1 Hz), 7.54-7.56 (d, 2H, *J* = 8.6 Hz), 7.58 (s, br, 1H), 7.81 (s, 1H), 7.81-7.83 (d, 2H, *J* = 8.7 Hz), 8.03-8.05 (d, 1H); ^{13}C NMR (100 MHz, $CDCl_3$): δ 108.5, 110.5, 114.3, 122.2, 124.1, 125.4, 125.6, 125.8, 127.3, 127.5, 127.8, 131.9, 133.1, 137.0, 141.9, 144.6, 145.8; MS (ESI^+): *m/z* = 381.7 $[M+H\ ^{79}Br]^+$, 383.6 $[M+H\ ^{81}Br]^+$; Anal. Calcd for $C_{19}H_{13}N_2SBr$: C, 59.85; H, 3.44; N, 7.35; S, 8.41 Found: C, 59.40; H, 3.34; N, 7.25; S, 8.44.

3. Results and Discussion

3.1. Preparation of arylstyrylimidazo[1,2-a]pyridine based chromophores

The aryl-substituted methylimidazo[1,2-a]pyridine derivatives **3a-c** were synthesized from 2-bromoacetophenone derivatives **2a**–**c** and 4-methyl-2-aminopyridine in good yields (Scheme 1). Light colorless and yellow crystals respectively for **3a** and **3b** of compounds suitable for X-ray diffraction analysis were obtained by slow evaporation from methanol (Figures S1 and S2, in Supporting information page S2). The imine derivatives **4a**–**f** were prepared by the reaction of aromatic aldehydes and the corresponding 4-chloroaniline derivative [54]. The arylstyrylimidazo[1,2-a]pyridine derivatives **5a**–**n** were obtained by the base-catalyzed condensation of the imine derivatives **4a**–**f** and the 2-aryl-substituted-7-methylimidazo[1,2-a]pyridine derivatives **3a**–**c** at 90 ^{o}C in DMF (Scheme 1). The experimental protocol is straightforward and offers easy access to a wide variety of arylstyrylimidazo[1,2-a]pyridines containing electron-donating groups in good yields. All compounds **5a**–**n** were characterized by NMR spectroscopy, mass spectrometry, and elemental analysis. NMR spectroscopy proved to be very useful to assess the configuration of the vinylic double bond. Within the limit of NMR-spectroscopic analysis only the formation of the *E* isomers could be detected. The assignment of the *E*-configuration of the vinylic double-bond was based on the analysis of the vicinal coupling constants of the olefinic protons, because the latter exhibit the characteristic coupling constant of $J \approx 16$ Hz. Although the arylstyrylimidazo[1,2-a]pyridines are persistent and can be stored in the solid state, the styryl double bond of the alkylamino-substituted derivatives isomerizes in solution, presumably induced by exposure to room light or sun light. The partial *E-Z* isomerization and amount of percent were detected by ^{1}H NMR

spectroscopic analysis of compound **5h** (Figures S3 and S4 in Supporting information page S3,S4).

Scheme 1 is here

3.2. Absorption and emission properties

The styryl derivatives **5a-n** are colored in solid state and in solution. To assess the solvatochromic behavior the absorption and emission data of the styryl derivatives were determined in DMSO, acetonitrile, THF, CH_2Cl_2 and toluene (Table 1).

Table 1 is here

The compounds **5a–n** show absorption maxima (λ_{max}) in the UV/visible region with long wavelength absorption maxima at 376-390 nm (in CH_2Cl_2). Although the compounds **5a**,**b** and **5i–n** exhibit two absorption bands in all solvents used, the derivatives **5c–h** showed just one absorption band (Figure 1). In addition, the compounds **5e-h** exhibit one shoulder in long wavelength in toulene used. The dyes which have two absorption bands or one absorption band with shoulder, may exhibit *E-Z* isomerization [26]. In addition these styryl derivatives are fluorescent (416–473 in CH_2Cl_2). Generally, the dyes **5c–n** show lower fluorescence quantum yields than derivatives **5a,b** with R^2 = H. It may be proposed that the relative low fluorescence quantum yields are the result of an photo-induced intramolecular electron transfer (PET) [55-57] reaction between the excited fluorophore (imidazopyridine ring as an electron acceptor) and the electron donating dialkylamino, thiomethyl, methoxy groups and thienyl ring. In general, larger Stokes shifts are obtained for alkylamino derivatives **5c-h** under investigation (e.g., **5d**: 5319 cm^{-1}; **5g**: 4972 cm^{-1} in CH_2Cl_2).

Regarding the absorption the compounds **5a–n** showed only weak solvatochromic properties. In contrast, all compounds exhibit fluorosolvatochromism, i.e. a bathochromic shift of the emission band was observed with increasing solvent polarity (Figure 1). Such a behavior is typical of donor-acceptor π systems that undergo an internal charge transfer upon excitation, [58] because the polar excited state is significantly stabilized by polar solvents.

Figure 1 is here

The absorption maxima of derivatives with an electron-donating substituent, such as the dialkylamino, methylsulfanyl and methoxy substituents, or of the thienylvinylimidazo[1,2-a]pyridines where the phenyl ring is substituted with the electron rich thiophene unit, showed significant bathochromic shifts as compared to the ones of the reference compounds **5a,b**. The same trend was observed in the emission spectra of compounds **5a–n**. The bathochromic shift is most likely the result of the more pronounced donor-acceptor interplay between the donor functionalities and the eletron-poor imidazopyridine ring. Notably, this effect is more dominant in compounds **5c–h** than for compounds **5i–n** as the former carry the stronger donor substituents. Hence, when the dialkylamino groups are attached at the *para* position of phenyl ring, a more pronounced donor-acceptor system is established between dialkylamino functionality and the imidazopyridine ring resulting in a larger red shift.

3.3. Acidochromic properties

Considering the alkaline functionality of the nitrogen atom of the dialkyl-aminophenyl and of the imidazopyridine ring we examined the dependence of the absorption and emission properties of the derivatives **5a**–**n** (Table 2). Most notably, the absorption and emission

properties of aminophenyl-substituted arylstyrylimidazo[1,2]pyridine derivatives **5c**–**h** change significantly upon protonation (Table 2).

Table 2 is here

The general trend shall be illustrated exemplarily with the representative derivative **5h**. Thus, the addition of trifluoroacetic acid (TFA) to a solution of **5h** in dichloromethane led to a shift of the absorption maximum from 381 nm to 418 nm (Figures 2 and 3).

Figures 2 and 3 are here

The observed bathochromic shift (37 nm) of the absorption maximum may be explained by initial protonation of the imidazopyridine ring that leads to an increased donor-acceptor interplay between the amino functionality and the imidazonium ion (Scheme 2).

Scheme 2 is here

Further addition of TFA (1 mM) to the solution of **5h** in dichloromethane led to a shift of the absorption maximum from 418 nm to 349 nm, i.e. a hypsochromic shift of 32 nm with respect to the neutral form **5h**. Apparantly, with excess of TFA the compound is also protonated at the amino-functionality which leads to a collapse of the donor-acceptor system (Scheme 2, Figure 4). The same hypsochromic shifts were observed for the dialkylamino-substituted derivatives **5c**–**g**, and such a phenomenon has been already observed upon protonation of alkylamino-substituted arylvinyldiazine derivatives [59].

Figure 4 is here

Upon adition of acid the emission properties of the derivatives **5a**–**n** also change significantly (Table 2). Hence, the emission intensity of **5i**–**n** was completely or partially quenched upon protonation, whereas the emission intensity of for **5c**–**h** increased in the presence of the acid. For example, upon addition of acid to **5h** in CH_2Cl_2 the fluorescence intensity increased 3 fold with a small red shift of the emission maxima from 457 nm to 465 nm (Figure 5,6). As discussed above the low emission quantum yield of the amino-substituted derivatives originates from a deactivating PIET between the amino functionality and the excited imidazopyridine unit. Therefore the light-up effect of **5c**–**h** on acidification is most likely the result of a suppressed PIET by protonation of the amino functionality [54].

Figure 5 and 6 are here

Conclusion

In summary, fourteen arylstyrylimidazo[1,2-a]pyridine-based donor-acceptor chromophores were prepared via facile methods. All chromophores have an *E*-configuration of the vinyl double bond as unequivocally shown by ^{1}H NMR spectroscopy. It was observed that the *E* isomers are stable in the solid state; however, the derivatives with strong electron donating dialkylamino substituents underwent partial *E*-*Z* isomerization in solution at room temperature. The synthesized all compounds exhibit fluorosolvatochromism, namely the emission band is red shifted with increasing solvent polarity.

The probes had high fluorescent in acidic media but low fluorescent in neutral environments. PIET is observed with addition excess of TFA to the solution of **5c-h** in dichloromethane. After double protonation of compounds **5c-h** light up effect is observed. This behavior may

be used for the development of light up probe for pH differences in biological and enviromental media.

Acknowledgements

This investigation was supported by The Scientific and Technological Research Council of Turkey (TUBITAK).

Supplementary material

The detailed spectroscopic data (Copies of ^{1}H and Mass spectra for all new compounds) of all new compounds are available. The crystallographic data for **3a** and **3b** can be seen therein. CCDC-984716 (**3a**) and 984220 (**3b**) contain the all supplementary crystallographic data for this paper. This data can be obtained free of charge from The Cambridge Crystallographic Data Centre viahttp://www.ccdc.cam.ac.

References

[1] Guo Z, Zhu W, Tian H. Dicyanomethylene-4*H*-pyran chromophores for OLED emitters, logic gates and optical chemosensors. Chem Commun 2012;48:6073-84.

[2] Guliyev R, Ozturk S, Kostereli Z, Akkaya EU. From Virtual to Physical: Integration of Chemical Logic Gates. Angew Chem Int Edit 2011;50:9826-31.

[3] Kim HN, Guo ZQ, ZhuWH, Yoon JY, Tian H. Recent progress on polymer-based fluorescent and colorimetric chemosensors. Chem Soc Rev 2011;40:79-93.

[4] Yang G, Yunxiang L, Wenxia G, Miaochang L, Jiuxi C,Yuefei H, Xiaobo H, Huayue W, Hui Li. D-p-A benzo[c][1,2,5]selenadiazole-based derivatives via an ethynylbridge: Photophysical properties, solvatochromism and applications as fluorescent sensors, Dyes Pigments 2015;112:105-15.

[5] (a) Haugland, RP. Handbook of Fluorescent Probes and Research Chemicals; Molecular Probes: Leiden, The Netherlands, 2002. (b) Nilsson KPR, Inganas O. Chip and solution detection of DNA hybridization using a luminescent zwitterionic polythiophene derivative. Nat Mater 2003;2:419-24 (c) Tian Y, Chen CY, Yang CC, Young AC, Jang SH, ChenWC, Jen AKY. 2-(2′-Hydroxyphenyl)benzoxazole-Containing Two-Photon-Absorbing Chromophores as Sensors for Zinc and Hydroxide Ions. Chem Mater 2008;20:1977-87.

[6] Chen H, Chung NN, Lemieux C, Zelent B, Vanderkooi JM, Gryczynski I, Wilkes BC, Schiller PW. [Aladan3]TIPP: a fluorescent delta-opioid antagonist with high delta-receptor binding affinity and delta selectivity. Biopolymers 2005;80:325-31.

[7] Vazquez ME, Blanco JB, Salvadori S, Trapella C, Argazzi R, Bryant S.D, Jinsmaa Y, Lazarus LH, Negri L, Giannini E, Lattanzi R, Colucci M, Balboni G. 6-*N*,*N*-Dimethylamino-2,3-naphthalimide: A New Environment-Sensitive Fluorescent Probe in δ- and μ-Selective Opioid Peptides. J Med Chem 2006;49:3653-58.

[8] Zhou G, Wang D, Ren Y, Yang S, Xu X, Shao Z, Cheng X, Zhao X, Fang Q, Jiang M. Temporal and spectral properties of picosecond two-photon pumped cavity lasing of an organic dye HEASPS. Appl Phys B-Laser O 2002;74:147-49.

[9] Vabre R, Legraverend M, Piguel S. Synthesis and evaluation of spectroscopic properties of newly synthesized pushepull 6-amino-8-styryl purines. Dyes Pigments 2014;105:145-51.

[10] Achelle S., Rodrıguez-Lopez J., Robin-le Guen F. Synthesis and Photophysical Studies of a Series of Quinazoline Chromophores, J Org Chem 2014 doi: 10.1021/jo501305h.

[11] Qin C, Zhang W, Wang Z, Zhou M, Wang X, Chen G. Optical properties of stilbene-type dyes containing various terminal donor and acceptor groups. Opt Mater 2008;30:1607-15.

[12] Ruland G, Gvishi R, Prasad PN. Multiphasic Nanostructured Composite: Multi-Dye Tunable Solid State Laser. J Am Chem Soc 1996;118:2985-91.

[13] Zhao CF, Gvishi R, Narang U, Ruland G, Prasad PN. Structures, Spectra, and Lasing Properties of New (Aminostyryl)pyridinium Laser Dyes. J Phys Chem 1996;100:4526-32.

[14] He GS, Bhawalkar JD, Zhao CF, Prasad PN. Optical limiting effect in a two-photon absorption dye doped solid matrix. Appl Phys Lett 1995;67:2433-35.

[15] Zheng Q, He G.S, Lin TC, Prasad PN. Synthesis and properties of substituted (*p*-aminostyryl)-1-(3-sulfooxypropyl)pyridinium inner salts as a new class of two-photon pumped lasing dyes. J Mater Chem 2003;13:2499-504.

[16] Abraham, U. An introduction to ultrathin organic films: From Langmuir-Blodgett to self-assembly; Academic Press: Boston, 1991.

[17] Messier J, Kajzar F, Prasad P, Eds. Organic molecules for nonlinear optics and photonics; Klumer Academic Publishers: Dordrecht, Boston, 1991.

[18] Chemla D.S, Zyss J. Nonlinear optical properties of organic molecules and crystals; Academic Press: Orlando, FL, 1987.

[19] Dörr H, Bouas-Laurent H. Photochromism-molecules and systems; Elsevier: Amsterdam, 1990.

[20] Clarke RJ, Kane DJ. Two Gears of Pumping by the Sodium Pump. Biophys J 2007;93: 4187-96.

[21] Clarke RJ, Apell HJ, Kong BY. Allosteric Effect of ATP on Na^+,K^+-ATPase Conformational Kinetics. Biochemistry 2007;46:7034-44.

[22] Jones MA, Bohn PW. Total Internal Reflection Fluorescence and Electrocapillary Investigations of Adsorption at a H_2O-Dichloroethane Electrochemical Interface. 1. Low-Frequency Behavior. Anal Chem 2000;72:3776-83.

[23] Zhang J, Davidson RM, Wei MD, Loew LM. Membrane Electric Properties by Combined Patch Clamp and Fluorescence Ratio Imaging in Single Neurons. Biophys J 1998; 74:48-53.

[24] Canepari M, Campani M, Spadavecchia L, Torre V. CCD imaging of the electrical activity in the leech nervous system. Eur Biophys J 1996;24:359-70.

[25] Cornelius F, Fedosova NU, Klodos I. E_2P Phosphoforms of Na,K-ATPase. II. Interaction of Substrate and Cation-Binding Sites in P_i Phosphorylation of Na,K-ATPase. Biochemistry 1998;37:16686-96.

[26] Deligeorgiev T, Vasilev A, Kaloyanova S, Vaquero JJ. Styryl dyes-synthesis and applications during the last 15 years. Color Technol 2010;126:55-80.

[27] Atilgan S, Ekmekci Z, Dogan A.L, Guc D, Akkaya E.U. Water soluble distyryl-boradiazaindacenes as efficient photosensitizers for photodynamic therapy. Chem Commun 2006;4398-400.

[28] Mashraqui SH, Ghorpade SS, Tripathi S, Britto S. A new indole incorporated chemosensor exhibiting selective colorimetric and fluorescence ratiometric signaling of fluoride. Tetrahedron Lett 2012;53:765-68.

[29] Shiraishi Y, Maehara H, Sugii T, Wang D, Hirai T. A BODIPY-indole conjugate as a colorimetric and fluorometric probe for selective fluoride anion detection. Tetrahedron Lett 2009;50: 4293-96.

[30] Bozdemir OA, Sozmen F, Buyukcakir O, Guliyev R, Cakmak Y, Akkaya EU. Reaction-Based Sensing of Fluoride Ions Using Built-In Triggers for Intramolecular Charge Transfer and Photoinduced Electron Transfer. Org Lett 2010;12:1400-03.

[31] Fan L, Fu YJ, Liu QL, Lu DT, Dong C, Shuang SM. Novel far-visible and near-infrared pH probes based on styrylcyanine for imaging intracellular pH in live cells. Chem Commun 2012;48:11202-04.

[32] Mishra A, Fischer M.K.R, Buerle P. Metal-Free Organic Dyes for Dye-Sensitized Solar Cells: From Structure: Property Relationships to Design Rules. Angew Chem Int Edit 2009; 48:2474-99.

[33] Gromov SP, Ushakov EN, Fedorova OA, Baskin II, Buevich AV, Elena NA, Alfimov MV, Johnels D, Edlund UG, Whitesell JK, Fox MA. Novel Photoswitchable Receptors: Synthesis and Cation-Induced Self-Assembly into Dimeric Complexes Leading to Stereospecific [2+2]-Photocycloaddition of Styryl Dyes Containing a 15-Crown-5 Ether Unit. J Org Chem 2003;68:6115-25.

[34] Matiukas A, Mitrea BG, Pertsov AM, Wuskell JP, Wei Mei-de, Watras J, Millard A.C, Loew LM. New near-infrared optical probes of cardiac electrical activity. Am J Phys Heart Circ Phys 2006;290:H2633-43.

[35] Kovalska VB, Losytskyy MY, Kryvorotenko DV, Balanda AO, Tokar VP, Yarmoluk SM. Synthesis of novel fluorescent styryl dyes based on the imidazo[1,2-*a*]pyridinium chromophore and their spectral-fluorescent properties in the presence of nucleic acids and proteins. Dyes Pigments 2006;68:39-45.

[36] Aranda AI, Achelle S, Hammerer F, Mahuteau-Betzer F, Teulade-Fichou MP. Vinyl-diazine triphenylamines and their N-methylated derivatives: Synthesis, photophysical properties and application for staining DNA. Dyes Pigments 2012;95:400-07.

[37] Xie X, Choi B, Largy E, Guillot R, Granzhan A, Teulade-Fichou M.P. Asymmetric Distyrylpyridinium Dyes as Red-Emitting Fluorescent Probes for Quadruplex DNA, Chem Eur J 2013;19:1214-26.

[38] Kamal A, Surendranadha RJ, Ramaiah MJ, Dastagiri D, Bharathi EV, Sagar MVP, Pushpavalli SNCVL, Ray P, Pal-Bhadra M. Design, synthesis and biological evaluation of imidazopyridine/pyrimidine-chalcone derivatives as potential anticancer agents. Med Chem Commun 2010;1:355-60.

[39] Elhakmaoui A, Gueiffier A, Milhavet JC, Blache Y, Chapat JP, Chavignon O, Teulade JC, Snoeck R, Andrei G, De Clercq E. Synthesis and antiviral activity of 3-substituted imidazo[1,2-*a*]pyridines. Bioorg Med Chem Lett 1994;4:1937.

[41] Lacerda RB, De Lima CK, Da Silva LL. Discovery of novel analgesic and anti-inflammatory 3-arylamine-imidazo[1,2-*a*]pyridine symbiotic prototypes. Bioorg Med Chem 2009;17:74-84.

[42] Almirante L, Polo L, Mugnaini A, Provinciali E, Rugarli P, Biancotti A, Gamba A, Murmann W. Derivatives of Imidazole. I. Synthesis and Reactions of Imidazo[1,2-α]pyridines with Analgesic, Antiinflammatory, Antipyretic, and Anticonvulsant Activity. J Med Chem 1965;8:305-12.

[43] Byth KF, Culshaw JD, Green S, Oakes S, Thomaset AP. Imidazo[1,2-*a*]pyridines. Part 2: SAR and optimisation of a potent and selective class of cyclin-dependent kinase inhibitors Bioorg Med Chem Lett 2004;14:2245-48.

[44] Crosby G.A, Demas J.N. Measurement of photoluminescence quantum yields. Rev J Phys Chem 1971; 75: 991-1024.

[45] B.Valeur, Molecular Fluorescence, Wiley-VCH Verlag GmbH, Weinheim, 2002.

[46] Rigaku/MSC, Inc.: 9009 new Trails Drive, The Woodlands, TX 77381.

[47] Sheldrick, G. M. SHELXS97 and SHELXL97; University of Göttingen: Germany, 1997

[48] Huang H, Ji X, Tang X, Zhang M, Li X, Jiang H. Conversion of Pyridine to Imidazo[1,2-*a*]pyridines by Copper-Catalyzed Aerobic Dehydrogenative Cyclization with Oxime Esters. Org Lett 2013;15:6254-57.

[49] Leopoldo M, Lacivita E, Passafiume E, Contino M, Colabufo NA, Berardi F, Perrone R. 4-[ω-[4-Arylpiperazin-1-yl]alkoxy]phenyl)imidazo[1,2-*a*]pyridine Derivatives: Fluorescent High-Affinity Dopamine D_3 Receptor Ligands as Potential Probes for Receptor Visualization. J Med Chem 2007;50:5043-47.

[50] Adib M, Mohamadi A, Sheikhi E, Ansari S, Bijanzadeh HR. Microwave-Assisted, One-Pot Reaction of Pyridines, α-Bromoketones and Ammonium Acetate: An Efficient and Simple Synthesis of Imidazo[1,2-*a*]-pyridines. Synlett 2010;11:1606-08.

[51] Naeimi H, Sharghi H, Salimi F, Rabiei K. Facile and efficient method for preparation of schiff bases catalyzed by P_2O_5/SiO_2 under free solvent conditions. Heteroatom Chem 2008;19:43-47.

[52] Mandhane PG, Joshi R.S, Nagargoje DR, Chate AV, Gill CH. Ultrasonic Promoted Synthesis and Antibacterial Screening of Some Novel Piperidine Incorporated α-Aminophosphonates. Phosphorus Sulfur 2011;186:149-58.

[53] Zhang F.G. 4-Chloro-*N*-[4-(diethylamino)benzylidene]aniline. Acta Cryst 2010;E66: o382.

[54] Pawhard JP, Siegrist AE. 11.Anil-Synthese. 16. Mitteilung. Über die Herstellung von styryl-derivaten des 2-phenyl-imidazo [1,2-*a*]pyridins. Helv Chim Acta 1978;61:129-41.

[55] Öztürk G, Karabıyık H, Aygün M, Alp S, Özçelik S. Tuning Photoinduced Intramolecular Electron Transfer by Electron Accepting and Donating Substituents in Oxazolones. J Fluoresc 2013; 23:733-44.

[56] Shane OM, O'Shea DF. Near-Infrared Sensing Properties of Dimethlyamino-Substituted BF_2-Azadipyrromethenes. Org Lett 2006;8:3493-96.

[57] de Silva AP, Moodyb TS, Wright GD. Fluorescent PET (Photoinduced Electron Transfer) sensors as potent analytical tools. Analyst 2009;134:2385-93.

[58] Fan J, Hu M, Zhan P. and Peng X. Energy transfer cassettes based on organic fluorophores: construction and applications in ratiometric sensing Chem Soc Rev 2013,42, 29-43.

[59] Achelle S, Barsella A, Baudequin C, Caro B, Robin-Le Guen F. Synthesis and Photophysical Investigation of a Series of Push–Pull Arylvinyldiazine Chromophores. J Org Chem 2012;77:4087-96.

Figure Captions

1. **Figure 1.** Absorption and emission spectra of compound **5h** in different solvents; absorption: *c* =10 μM; emission: *c*: 1.0 μM.
2. **Figure 2.** Spectrophotometric titration of TFA to compound **5h** (10 μM) in CH_2Cl_2. Arrows indicate the increase and decrease of the absorbance intensity upon addition 1 mM TFA in CH_2Cl_2.
3. **Figure 3.** Pictures of absorption and emission color of **5h** in CH_2Cl_2 solutions (*c* = 10 μM; λ_{ex} = 365 nm) in the absence (right) presence (left) of 1 mM TFA in CH_2Cl_2.
4. **Figure 4.** Spectrophotometric titration of TFA to compound **5h** (10 μM) in CH_2Cl_2. Arrows indicate the increase and decrease of the absorbance intensity upon addition 1 mM TFA in CH_2Cl_2.
5. **Figure 5**. Spectrofluorimetric titration of (10 μM) **5h** in CH_2Cl_2. Arrow indicate the increase of the fluorescence intensity upon addition 1 M TFA in CH_2Cl_2
6. **Figure 6.** Pictures of emission color of **5h** (10 μM) at neutral (left) and acidic (right) conditions (λ_{ex} = 365 nm).

Scheme Captions

1. **Scheme 1.** Synthesis of arylstyrylimidazo[1,2-a]pyridine derivatives **5a-n**.
2. **Scheme 2.** Prototropic equilibria of **5h**.

Table Captions

1. **Table 1.** Photophysical data of arylstyrylimidazo[1,2-a]pyridine based dyes **5a–n**
2. **Table 2.** pH-Dependent Absorption and Emission Properties of arylstyrylimidazo[1,2-a]pyridine based dyes **5a-n.**

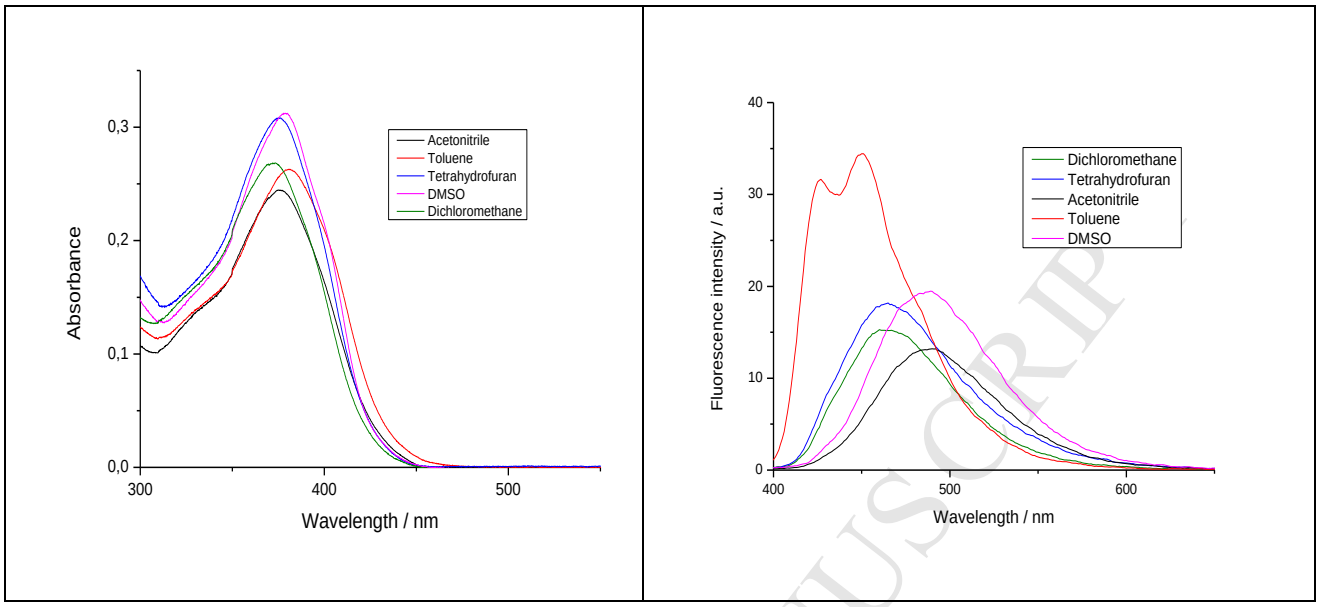

Figure 1. Absorption and emission spectra of compound **5h** in different solvents; absorption: *c* =10 μM; emission: *c*: 1.0 μM.

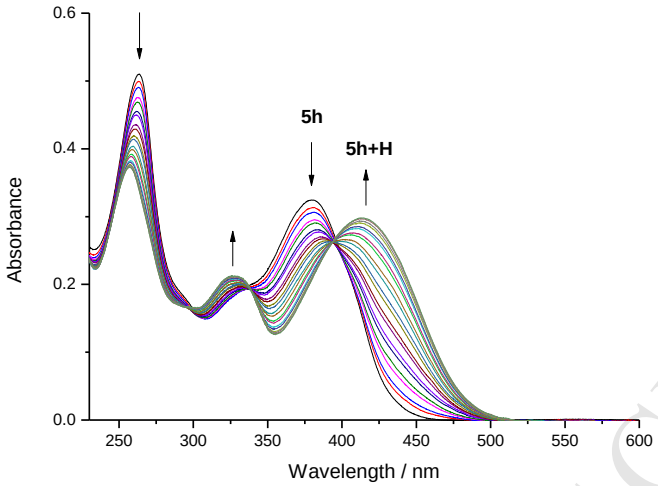

Figure 2. Spectrophotometric titration of TFA to compound **5h** (10 μM) in CH_2Cl_2. Arrows indicate the increase and decrease of the absorbance intensity upon addition 1 mM TFA in CH_2Cl_2.

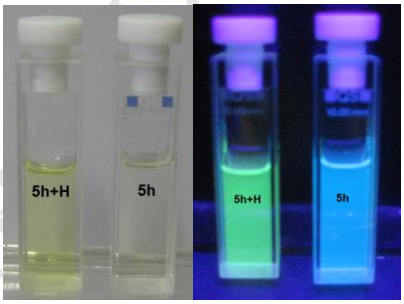

Figure 3. Pictures of absorption and emission color of **5h** in CH_2Cl_2 solutions (c = 10 μM; λ_{ex} = 365 nm) in the absence (right) presence (left) of 1 mM TFA in CH_2Cl_2.

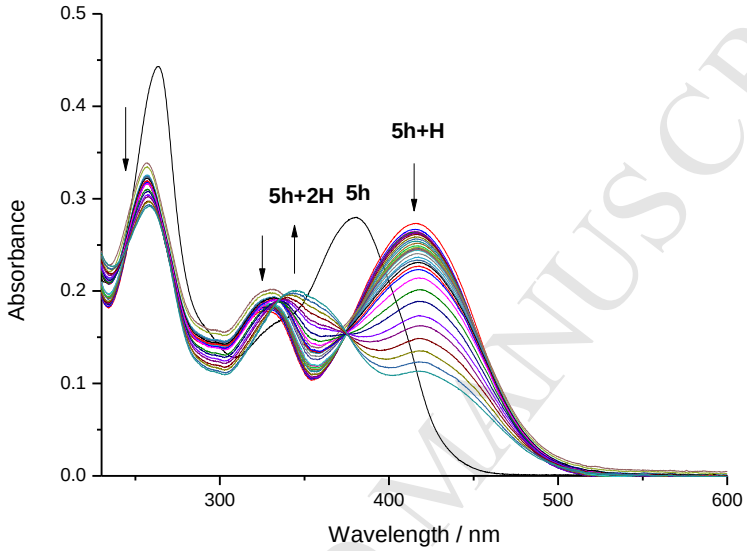

Figure 4. Spectrophotometric titration of TFA to compound **5h** (10 μM) in CH_2Cl_2. Arrows indicate the increase and decrease of the absorbance intensity upon addition 1 mM TFA in CH_2Cl_2.

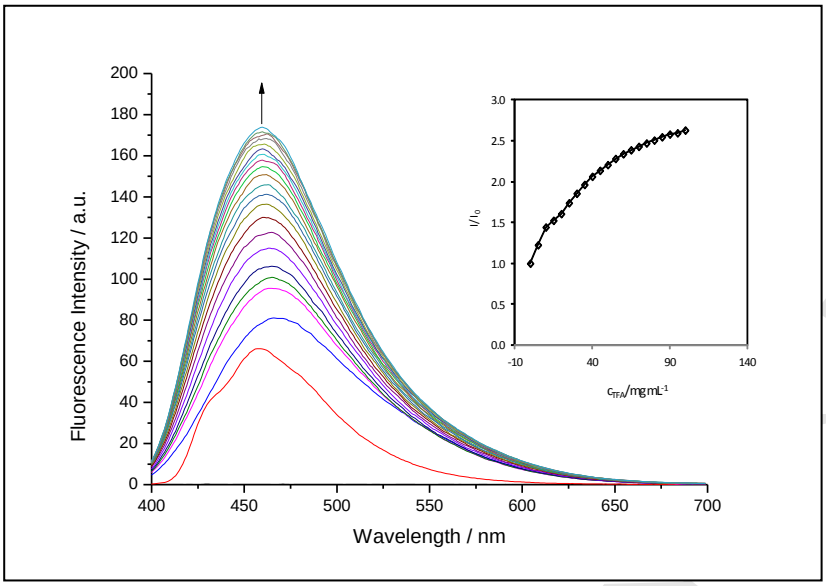

Figure 5. Spectrofluorimetric titration of (10 μM) **5h** in CH_2Cl_2. Arrow indicate the increase of the fluorescence intensity upon addition 1 M TFA in CH_2Cl_2

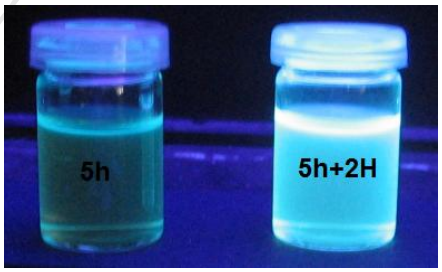

Figure 6. Pictures of emission color of **5h** (10 μM) at neutral (left) and acidic (right) conditions (λ_{ex} = 365 nm).

Figure

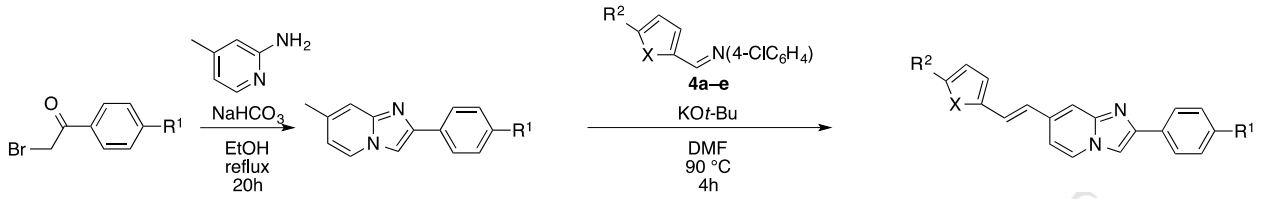

2a: R^1 = H
2b: R^1 = OMe
2c: R^1 = Br

3a: R^1 = H
3b: R^1 = OMe
3c: R^1 = Br

4a: R^2 = H; X = CH=CH
4b: R^2 = $N(CH_2)_5$; X = CH=CH
4c: R^2 = NEt_2; X = CH=CH
4d: R^2 = NMe_2; X = CH=CH
4e: R^2 = SMe; X = CH=CH
4d: R^2 = OMe; X = CH=CH
4e: R^2 = H; X = S

5a: R^1 = H; R^2 = H; X = CH=CH
5b: R^1 = OMe; R^2 = H; X = CH=CH
5c: R^1 = H, R^2 = $N(CH_2)_5$; X = CH=CH
5d: R^1 = OMe, R^2 = $N(CH_2)_5$; X = CH=CH
5e: R^1 = H; R^2 = NEt_2; X = CH=CH
5f: R^1 = OMe; R^2 = NEt_2; X = CH=CH
5g: R^1 = H; R^2 = NMe_2; X = CH=CH
5h: R^1 = OMe; R^2 = NMe_2; X = CH=CH
5i: R^1 = H; R^2 = SMe; X = CH=CH
5j: R^1 = OMe; R^2 = SMe; X = CH=CH
5k: R^1 = H; R^2 = OMe; X = CH=CH
5l: R^1 = OMe; R^2 = OMe; X = CH=CH
5m: R^1 = Br; R^2 = H; X = S
5n: R^1 = OMe; R^2 = H; X = S

Scheme 1. Synthesis of arylstyrylimidazo[1,2-a]pyridine derivatives **5a-n**.

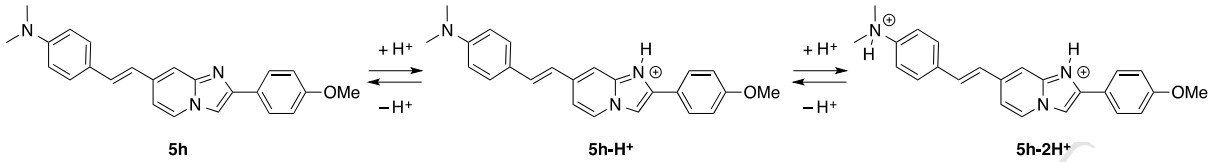

Scheme 2. Prototropic equilibria of **5h**.

Table 1. Photophysical data of arylstyrylimidazo[1,2-a]pyridine based dyes **5a–n**

Dye	DMSO				Acetonitrile				THF				CH_2Cl_2				Toluene			
	$^{a}\lambda_{abs}$ (nm) (log ε^{b})	$^{c}\lambda_{fl}$ (nm)	$^{d}\varphi_{fl}$	Stokes Shift, cm^{-1}	$^{a}\lambda_{abs}$ (nm) (log ε^{b})	$^{c}\lambda_{fl}$ (nm)	$^{d}\varphi_{fl}$	Stokes Shift, cm^{-1}	$^{a}\lambda_{abs}$ (nm) (log ε^{b})	$^{c}\lambda_{fl}$ (nm)	$^{d}\varphi_{fl}$	Stokes Shift, cm^{-1}	$^{a}\lambda_{abs}$ (nm) (log ε^{b})	$^{c}\lambda_{fl}$ (nm)	$^{d}\varphi_{fl}$	Stokes Shift, cm^{-1}	$^{a}\lambda_{abs}$ (nm) (log ε^{b})	$^{c}\lambda_{fl}$ (nm)	$^{d}\varphi_{fl}$	Stokes Shift, cm^{-1}
5a	361(4.42), 379(4.37)	425	0.33	2856	355(4.41), 372(4.36)	418	0.28	2958	359(4.46), 377(4.42)	416	0.28	2487	358(4.30), 376(4.24)	416	0.28	2557	361(4.38), 380(4.33)	397,418	0.25	2392
5b	362(4.46), 382(4.41)	438	0.33	3350	360(4.44), 375(4.39)	430	0.27	3411	362(4.40), 381(4.35)	426	0.26	2773	362(4.45), 380(4.40)	426	0.28	2842	366(4.38), 384(4.34)	425	0.26	2512
5c	380 (4.41)	491	0.21	5949	376 (4.34)	482	0.06	5849	374 (4.44)	463	0.12	5140	372 (4.55)	434	0.05	3840	378 (4.49)	435(sh.),456	0.24	4525
5d	380 (4.42)	491	0.14	5949	372 (4.43)	488	0.17	6390	375 (4.49)	470	0.11	5390	376 (4.39)	470	0.12	5319	378 (4.49)	435,456	0.17	4525
5e	391 (4.47)	489	0.05	5125	384 (4.52)	486	0.05	5466	384 (4.51)	462	0.03	4397	387 (4.59)	466	0.02	4381	387(407 sh.) (4.54)	434,457	0.04	3958
5f	391 (4.39)	486	0.12	4999	376 (4.41)	485	0.06	5892	385 (4.44)	468	0.08	4607	386 (4.30)	473	0.06	4765	388(409 sh.) (4.47)	434,457	0.14	3891
5g	386 (4.43)	490	0.18	5499	376 (4.34)	482	0.06	5849	379 (4.47)	459	0.07	4598	379 (4.32)	467	0.06	4972	379 (428)	431,453	0.15	4310
5h	382 (4.48)	489	0.10	5728	376 (4.41)	485	0.06	5977	380 (4.47)	463	0.09	4718	381 (4.43)	460	0.07	4508	384 (402 sh.) (4.44)	429,453	0.16	3967
5i	371(4.64), 391(4.57)	431	0.25	2374	365(4.64), 384(4.58)	423	0.13	2401	369(4.64), 388(4.58)	426	0.20	2299	368(4.68), 388(4.61)	426	0.22	2299	371(4.60), 391(4.54)	428	0.15	2211
5j	375(4.39), 394(4.34)	441	0.21	2705	369(4.55), 387(4.51)	433	0.16	2745	372(4.71) ,392(4.68)	432	0.21	2362	372(4.69), 390(4.64)	433	0.16	2546	375(4.58), 395(4.54)	411,434	0.16	2275
5k	365(4.58), 384(4. 54)	423	0.24	2401	359(4.56), 377(4.50)	416	0.13	2487	362(4.59), 381(4.56)	416	0.20	2208	362(4.57), 381(4.52)	418	0.22	2323	364(4.51), 383(4.47)	419	0.15	2243
5l	368(4.58), 386(4.55)	429	0.33	2596	362(4.50), 380(4.45)	423	0.31	2675	365(4.57), 384(4.53)	402,424	0.29	2457	365(4.55), 383(4.50)	405sh, 424	0.29	2524	368(4.52), 387(4.49)	401,424	0.22	2255
5m	373(4.43), 392(4.37)	432	0.07	2362	365(4.25), 385(4.14)	424	0.07	2389	369(4.47), 389(4.39)	425	0.09	2178	369(4.54), 388(4.45)	425	0.08	2244	372(4.29), 391(4.21)	427	0.07	2156
5n	372(4.39), 393(4.30)	432	0.12	2297	365(4.37), 385(4.29)	426	0.13	2499	369(4.40), 389(4.32)	427	0.10	2288	368(4.29), 387(4.13)	426	0.12	2366	372(4.36), 391(4.26)	429	0.12	2265

[a]Long wavelength absorption maximum, in nm; c= 10 μ M.
[b]**ε** = molar absorption coefficient, $cm^{-1}M^{-1}$.
[c]Fluorescence maximum, in nm;c= 1-5 μ M;
[d]Fluorescence quantum yield relative to Coumarin 1 (0.78) in ethanol [44,45].

Table 2. pH-Dependent Absorption and Emission Properties of arylstyrylimidazo[1,2-a]pyridine based dyes **5a–n.**

Dyes	UV/vis (TFA 0.1 M in CH_2Cl_2) λ_{max} (nm)	FL (TFA 0.1 M in CH_2Cl_2) λ_{max} (nm)	Stokes shift cm^{-1}
5a	354	410	3858
5b	362	433	4530
5c	349	406,581	11442
5d	357	470	6735
5e	345	425	5456
5f	357	453	5936
5g	338	405,554	11535
5h	355	465	6335
5i	387	488[a]	5348
5j	385	484[a]	5313
5k	375	-[b]	-
5l	380	-[b]	-
5m	375	-[b]	-
5n	384	-[b]	-

[a]Low fluorescence intensity, [b]Too low to be determined

Supporting Information for:

Synthesis and photophysical properties of fluorescent arylstyrylimidazo[1,2-a]pyridine-based donor-acceptor chromophores

Zeynel Seferoğlu[a,b] *, Heiko Ihmels[b] and Ertan Şahin[c]

[a]*Gazi University, Department of Chemistry, 06500 Ankara, Turkey*

[b]*University of Siegen, Organic Chemistry II, Adolf-Reichwein-Str. 2, D-57068 Siegen, Germany*

[c]*Atatürk University, Department of Chemistry, Erzurum, Turkey*

Corresponding author Tel.: +90 312 2021525; fax: +90 312 2122279

**E-mail addresses*: znseferoglu@gazi.edu.tr (Z. Seferoğlu)

Contents

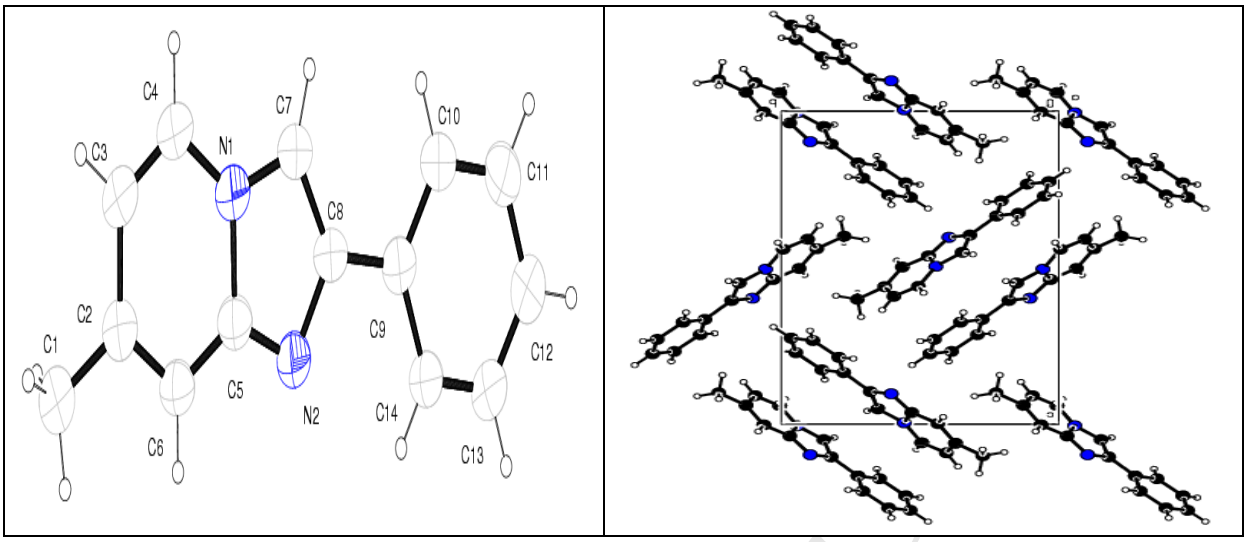

Figure S1. Structure of **3a** in the solid state and partial packing diagram.

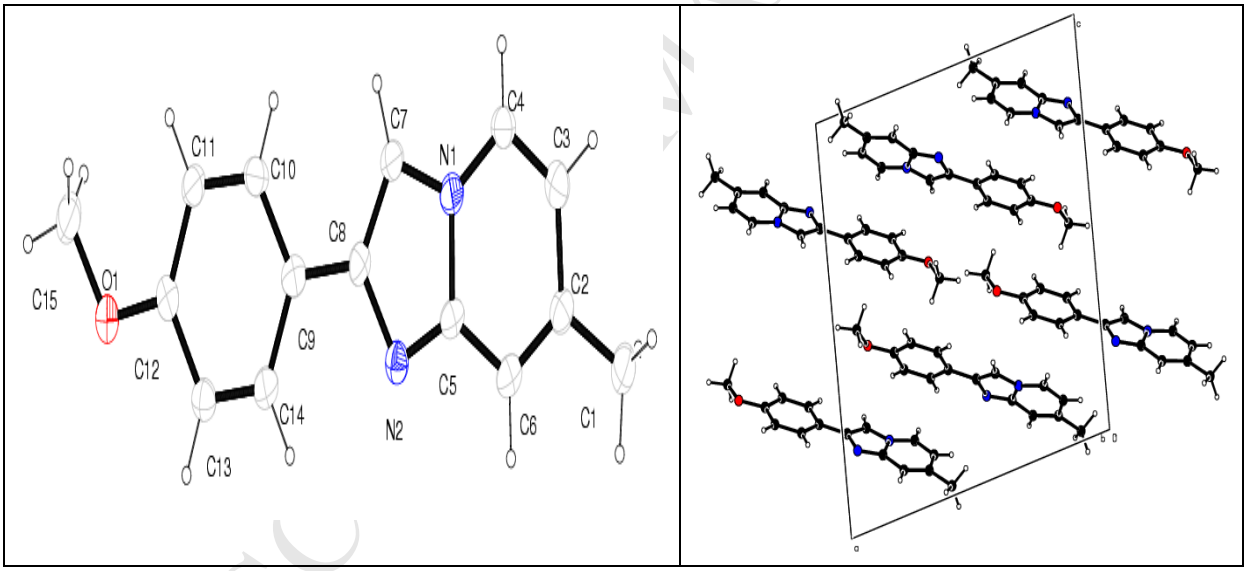

Figure S2. Structure of **3b** in the solid state and partial packing diagram.

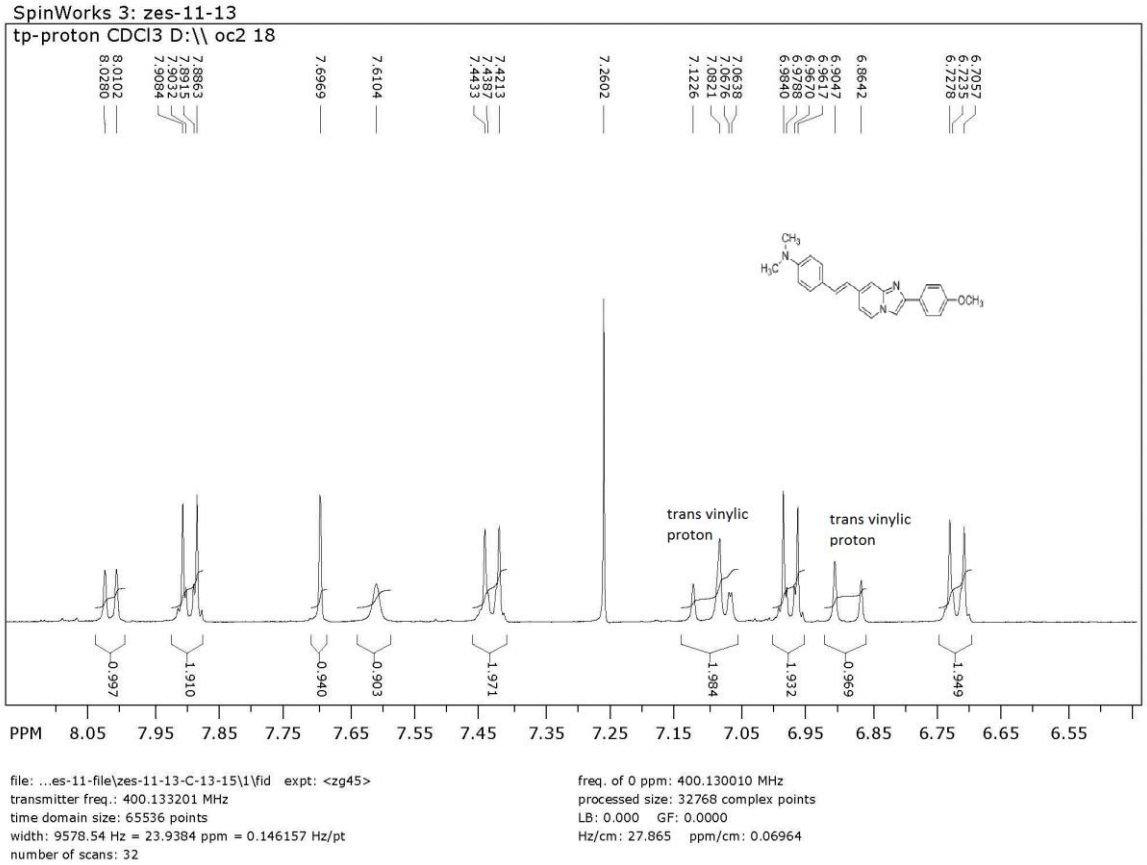

Figure S3. ^{1}H NMR spectrum of **5h** in $CDCl_3$

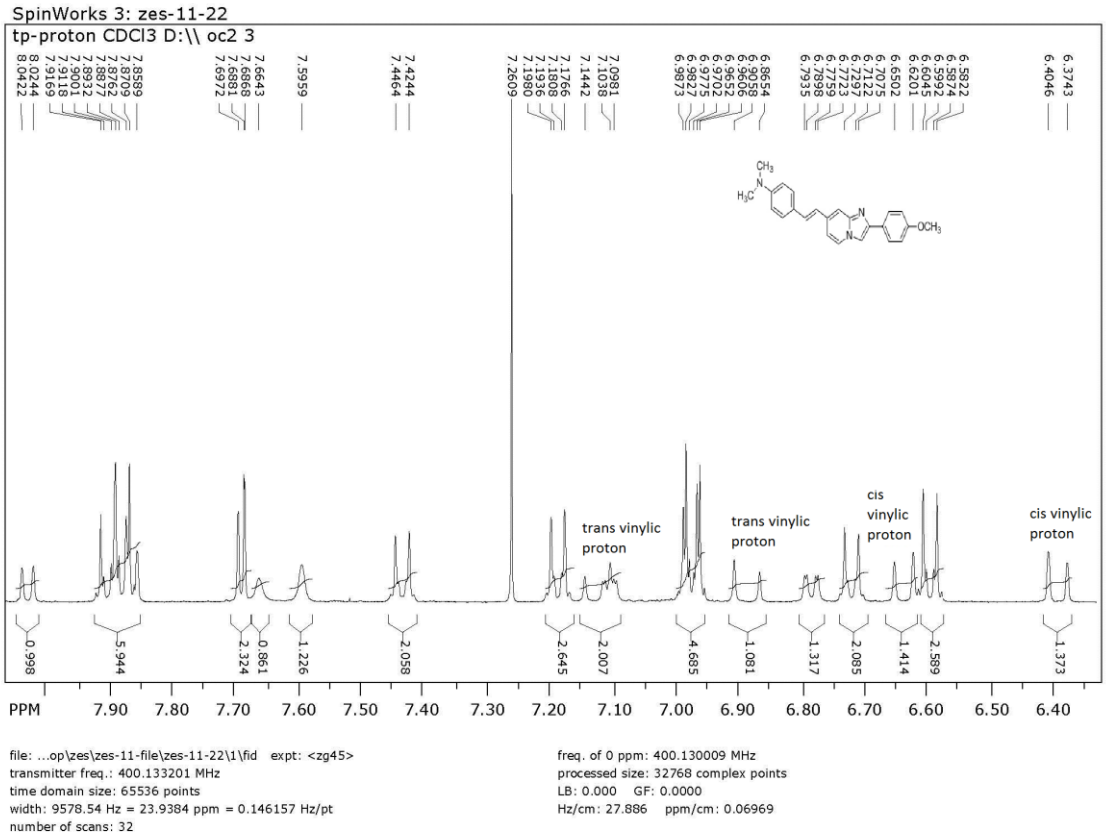

Figure S4. ^{1}H NMR spectrum of **5h** in $CDCl_3$ after keep in lab at room temperature for one day.

Table S1. Crystallographic data and structure refinement for **3a** and **3b**.

	3a	**3b**
Empirical formula	$C_{14}H_{12}N_2$	$C_{15}H_{14}N_2O$
Formula weight	208.26	238.28
Crystal dimensions (mm)	0.11x0.12x0.18	0.12x0.13x0.20
Temperature (K)	294	294
Crystal system	orthorhombic	monoclinic
Space group	$P2_12_12_1$	$P2_1/a$
a (Å)	5.846(3)	13.661 (5)
b (Å)	11.037(4)	5.813(2)
c (Å)	16.779(5)	15.689(5)
β (º)	90.00	100.86(3)
Volume ($Å^3$)	1082.6(8)	1223.6(7)
Z	4	4
D_{calc} (g cm^{-3})	1.278	1.294
θ_{max} (º)	26.45	26.4
μ (mm^{-1})	0.077	0.083
No. of reflections measured	22764	19838
No. of. Reflections observed [$I>2\sigma(I)$] / R_{int}	1629/0.057	2126/0.112
No. of parameters	147	165
R / R_w values	0.058 / 0.174	0.088 / 0.231
Goodness of Fit	1.49	1.036
Largest diff. peak and hole(e $Å^{-3}$)	0.189/ - 0.130	0.223/ - 0.297

^{1}H-NMR and Mass Spectra of Synthesized Compounds:

^{1}H-NMR Spectrum of 5a

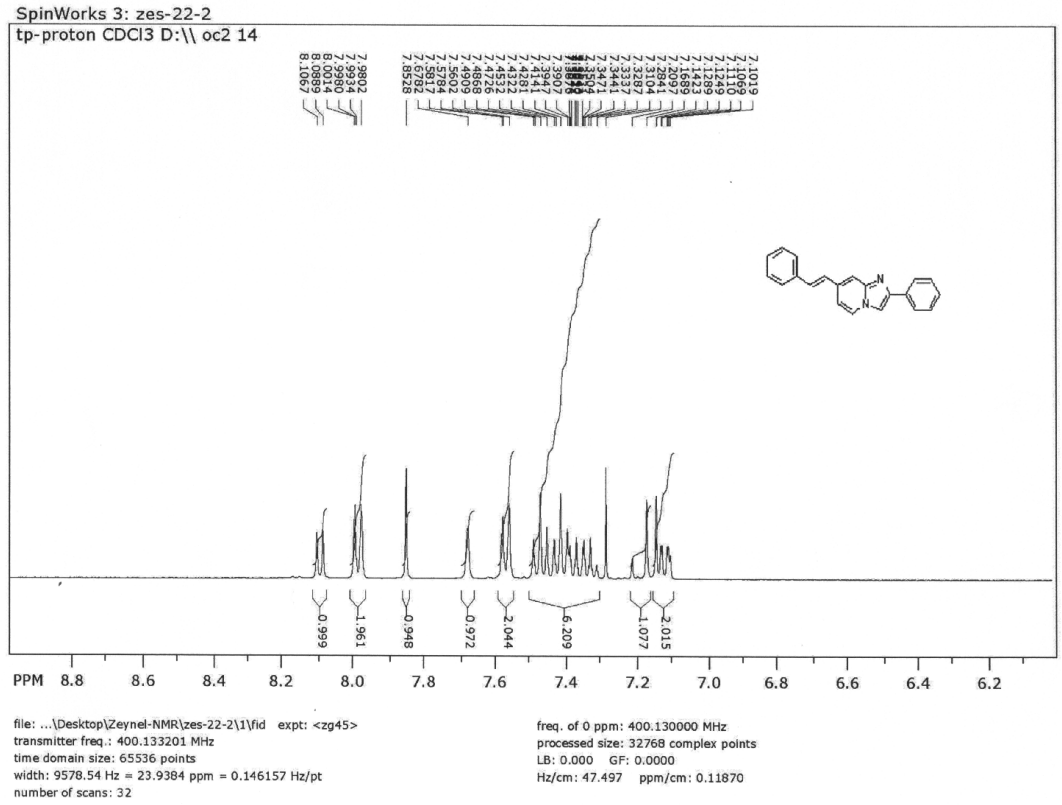

Mass Spectrum of 5a

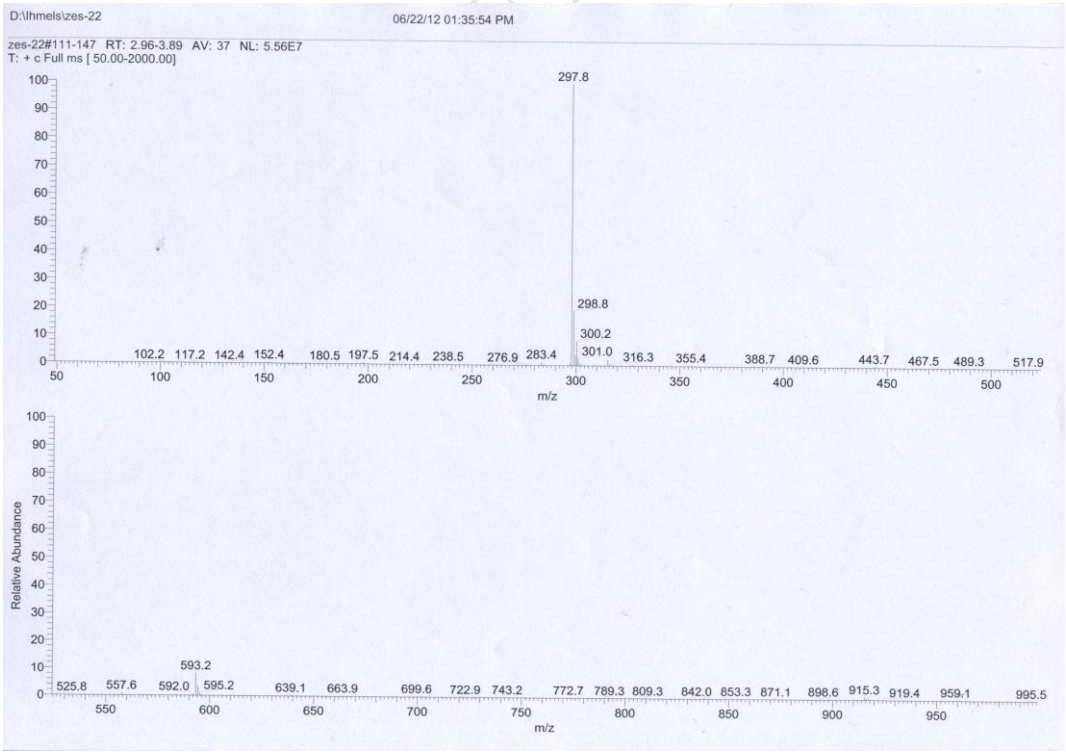

^{1}H-NMR Spectrum of 5b

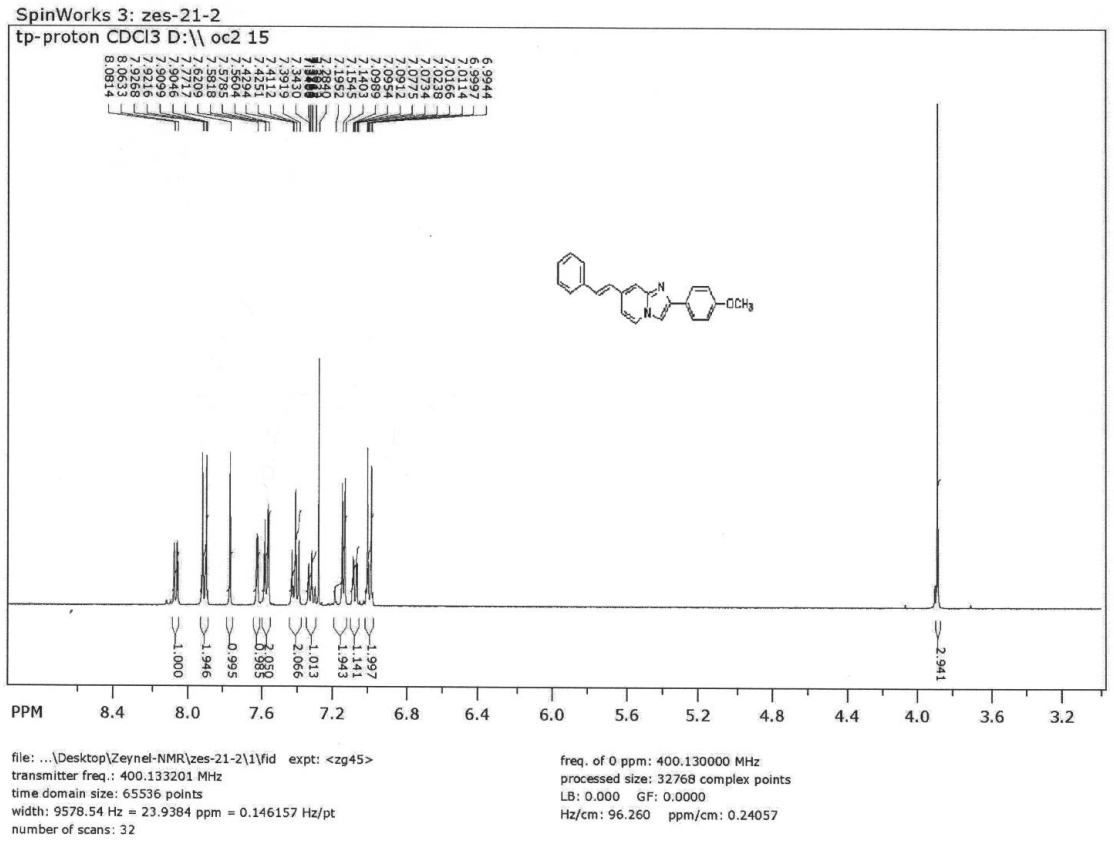

Mass Spectrum of 5b

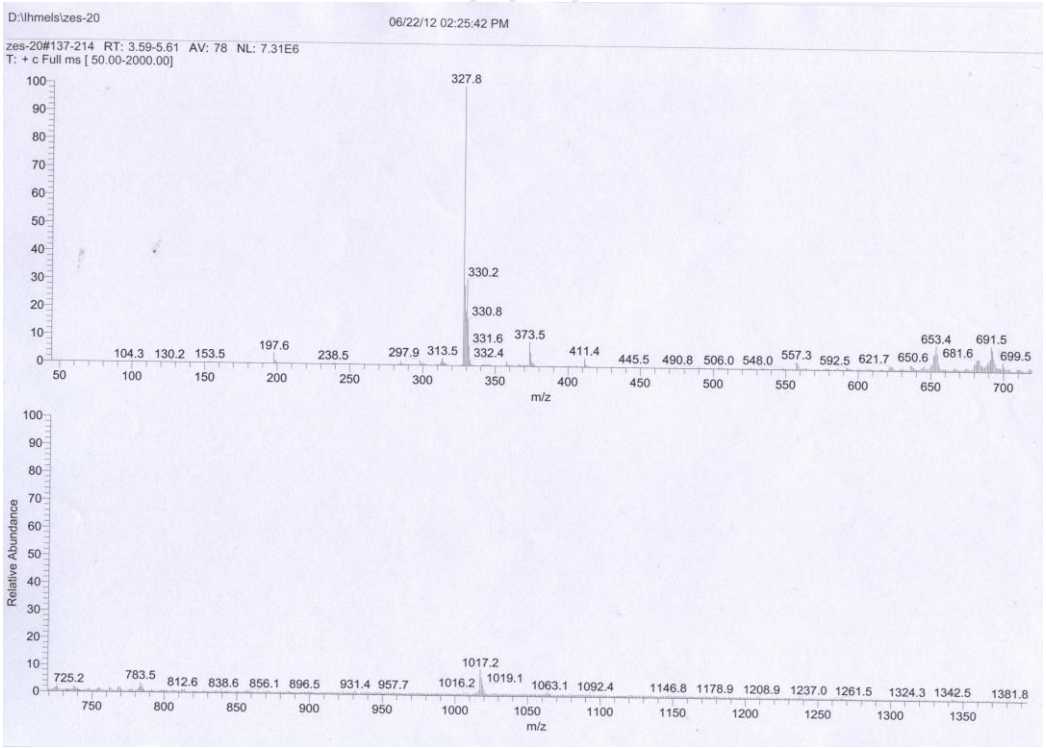

^{1}H-NMR Spectrum of 5c

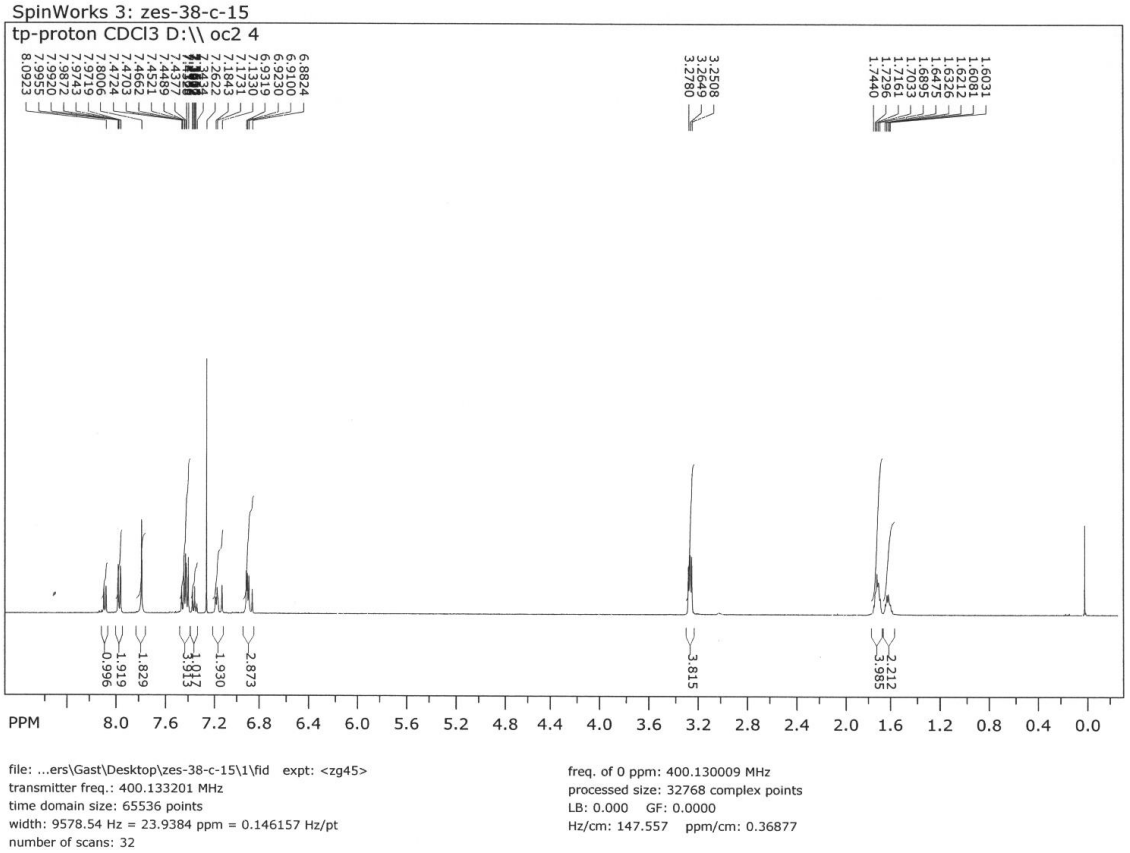

Mass Spectrum of 5c

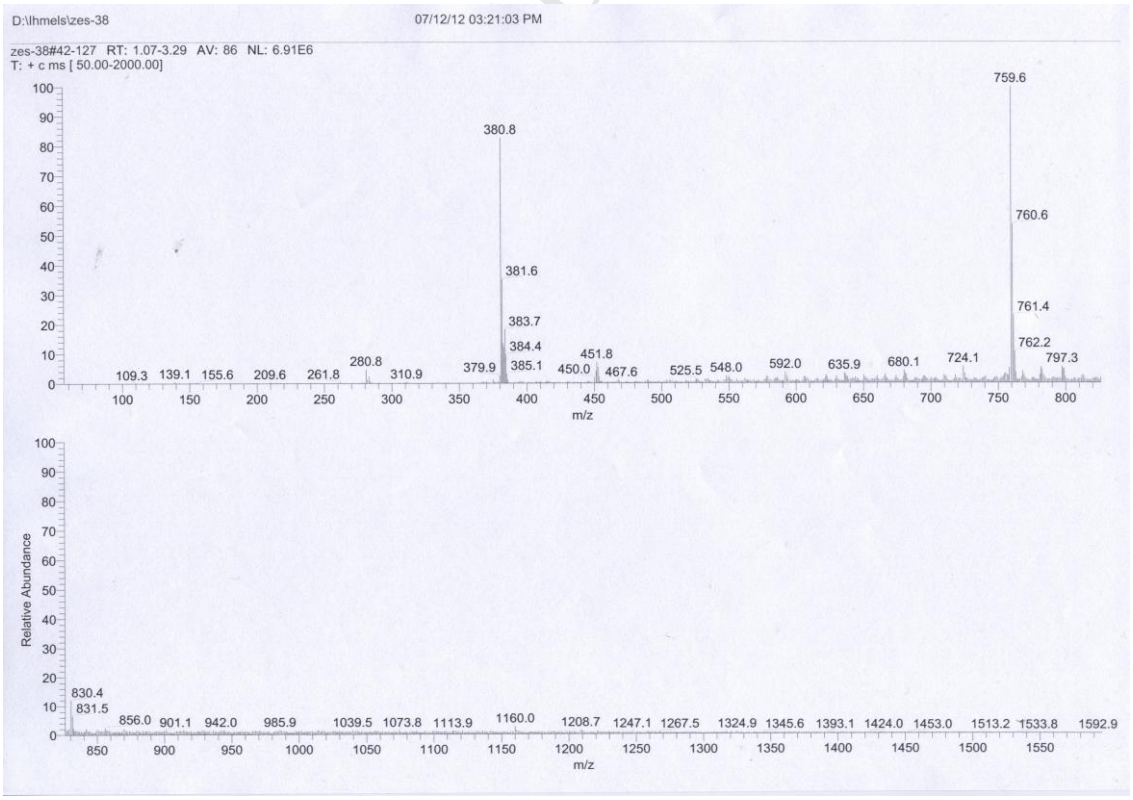

^{1}H-NMR Spectrum of 5d

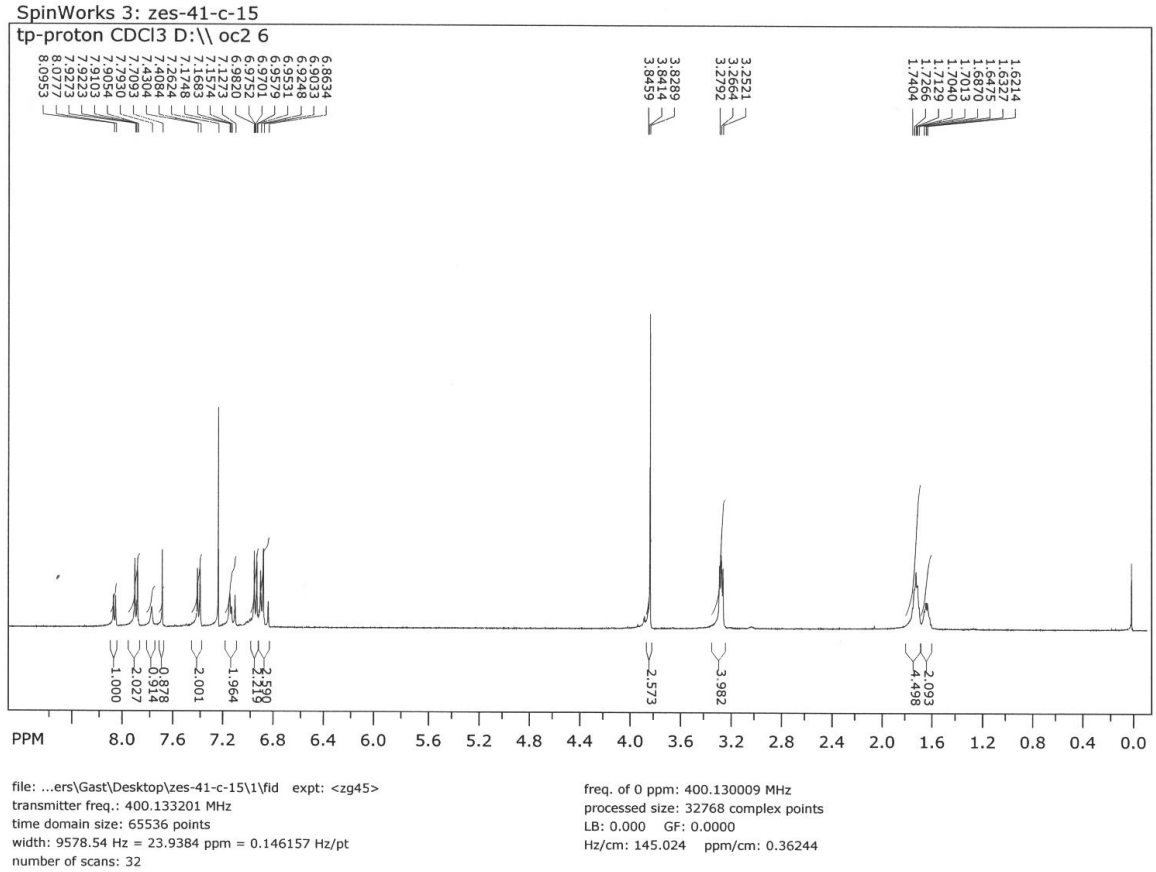

file: ...ers\Gast\Desktop\zes-41-c-15\1\fid expt: <zg45>
transmitter freq.: 400.133201 MHz
time domain size: 65536 points
width: 9578.54 Hz = 23.9384 ppm = 0.146157 Hz/pt
number of scans: 32

freq. of 0 ppm: 400.130009 MHz
processed size: 32768 complex points
LB: 0.000 GF: 0.0000
Hz/cm: 145.024 ppm/cm: 0.36244

Mass Spectrum of 5d

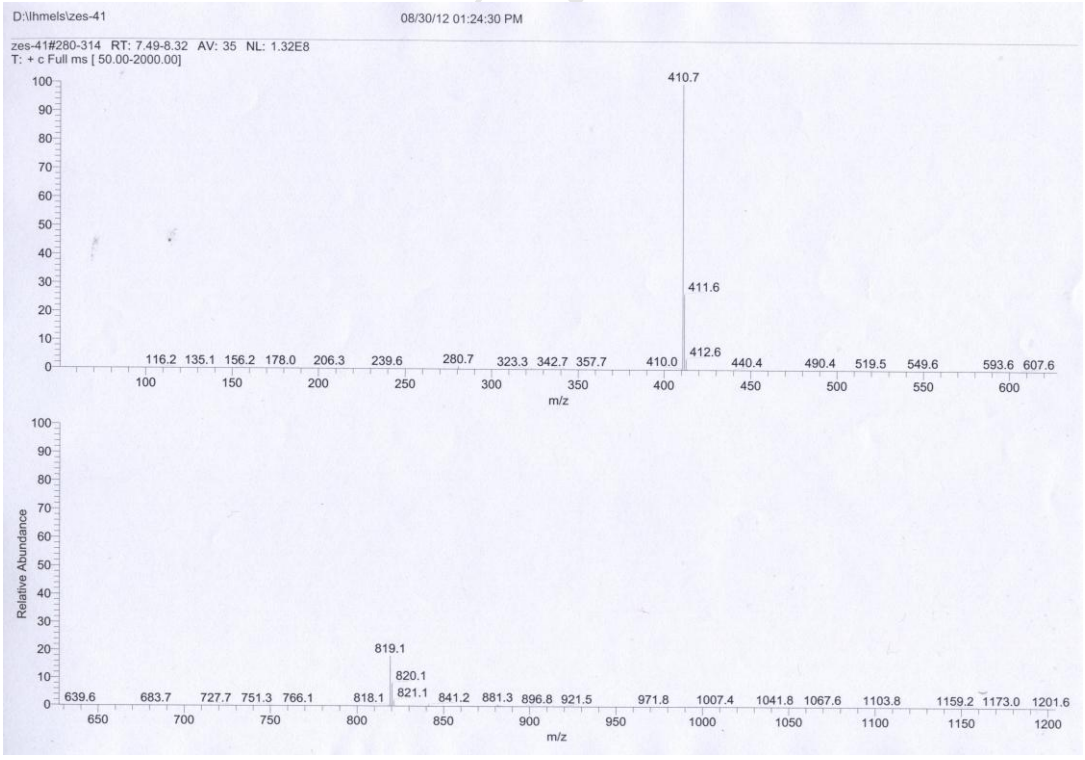

^{1}H-NMR Spectrum of 5e

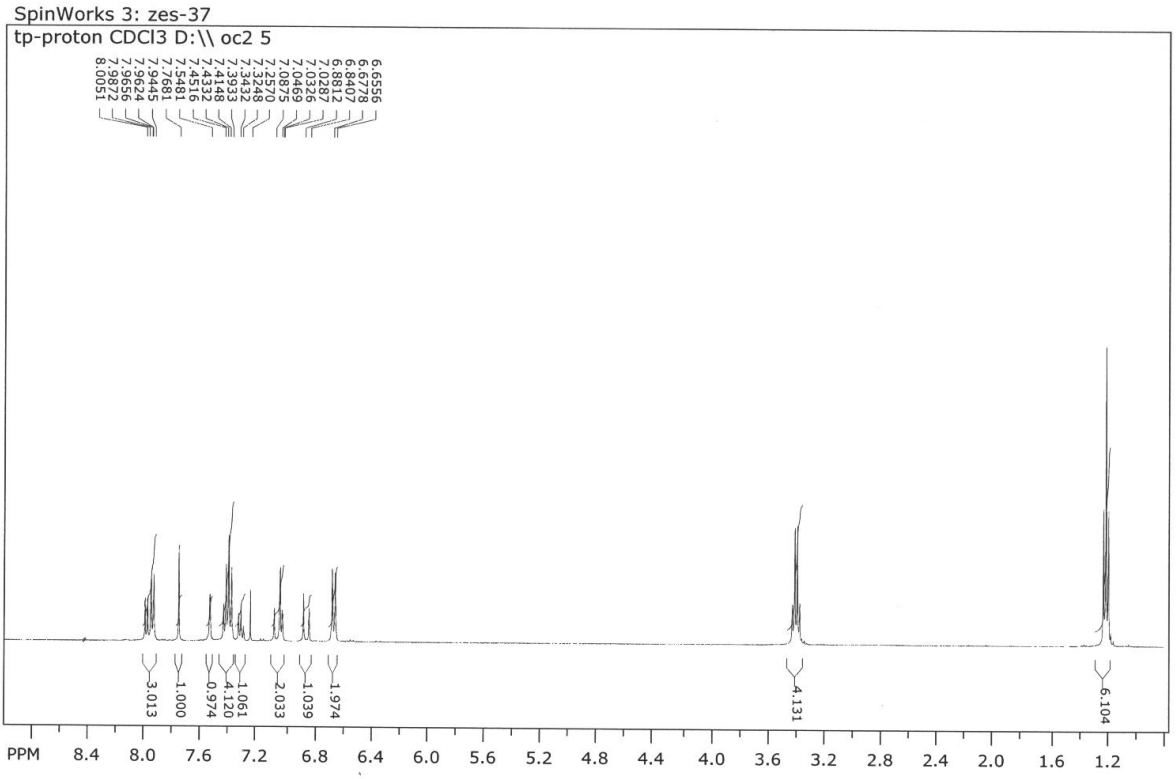

file: ...sers\Gast\Desktop\zes\zes-37\1\fid expt: <zg45>
transmitter freq.: 400.133201 MHz
time domain size: 65536 points
width: 9578.54 Hz = 23.9384 ppm = 0.146157 Hz/pt
number of scans: 32

freq. of 0 ppm: 400.130011 MHz
processed size: 32768 complex points
LB: 0.000 GF: 0.0000
Hz/cm: 131.725 ppm/cm: 0.32920

Mass Spectrum of 5e

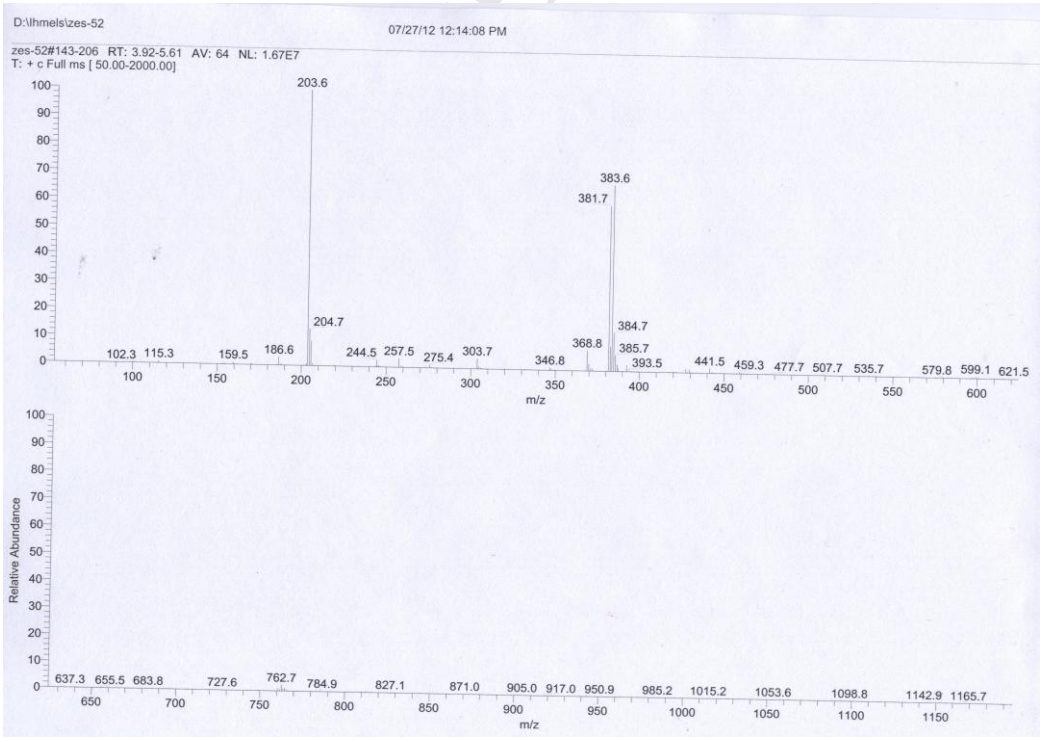

^{1}H-NMR Spectrum of 5f

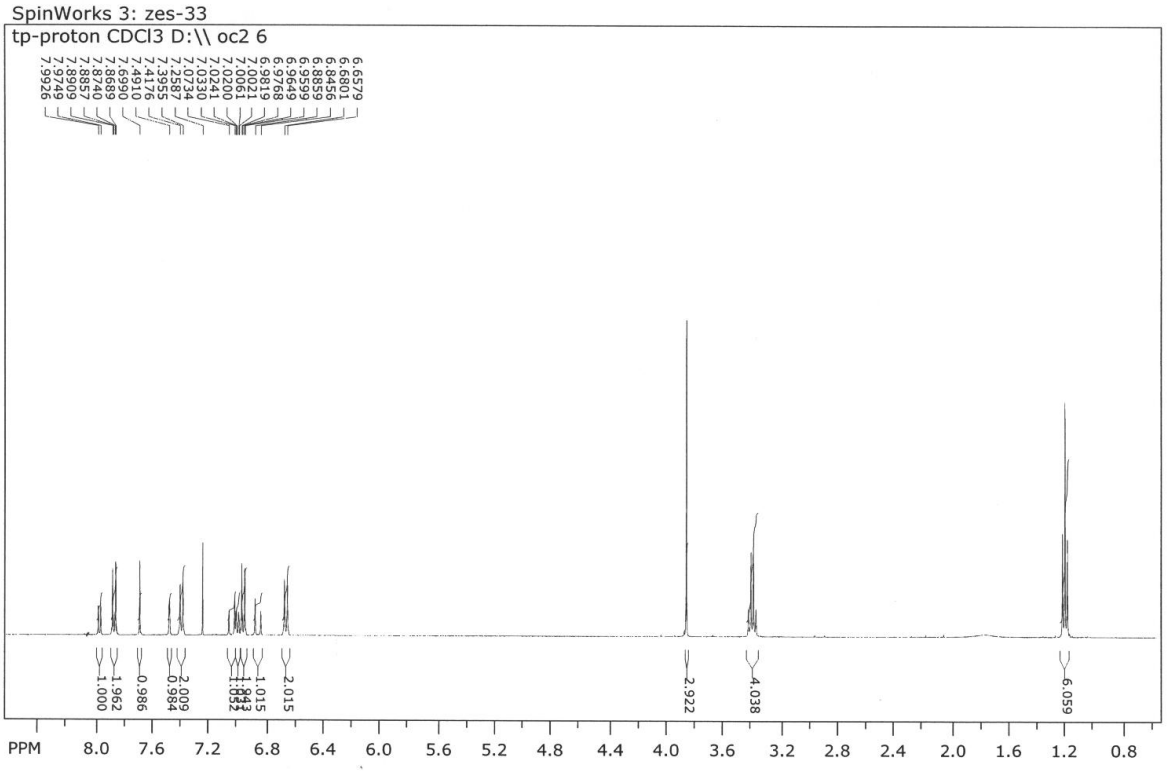

file: ...sers\Gast\Desktop\zes\zes-33\1\fid expt: <zg45>
transmitter freq.: 400.133201 MHz
time domain size: 65536 points
width: 9578.54 Hz = 23.9384 ppm = 0.146157 Hz/pt
number of scans: 32

freq. of 0 ppm: 400.130010 MHz
processed size: 32768 complex points
LB: 0.000 GF: 0.0000
Hz/cm: 129.825 ppm/cm: 0.32445

Mass Spectrum of 5f

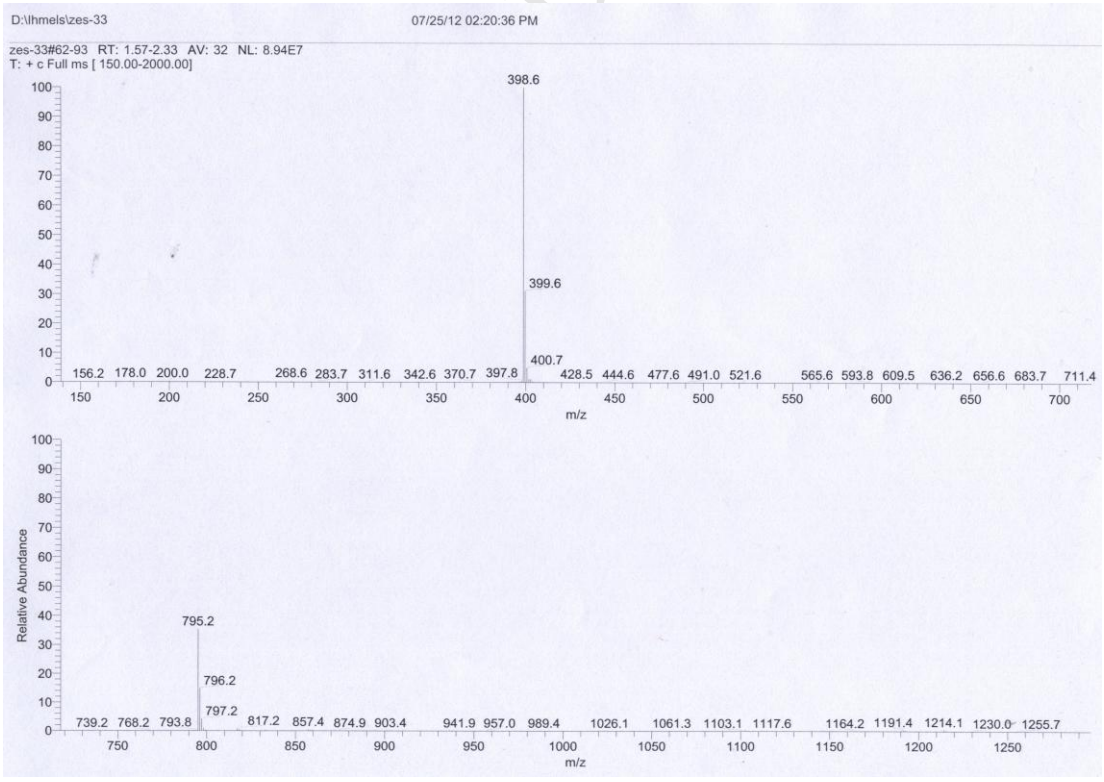

^{1}H-NMR Spectrum of 5g

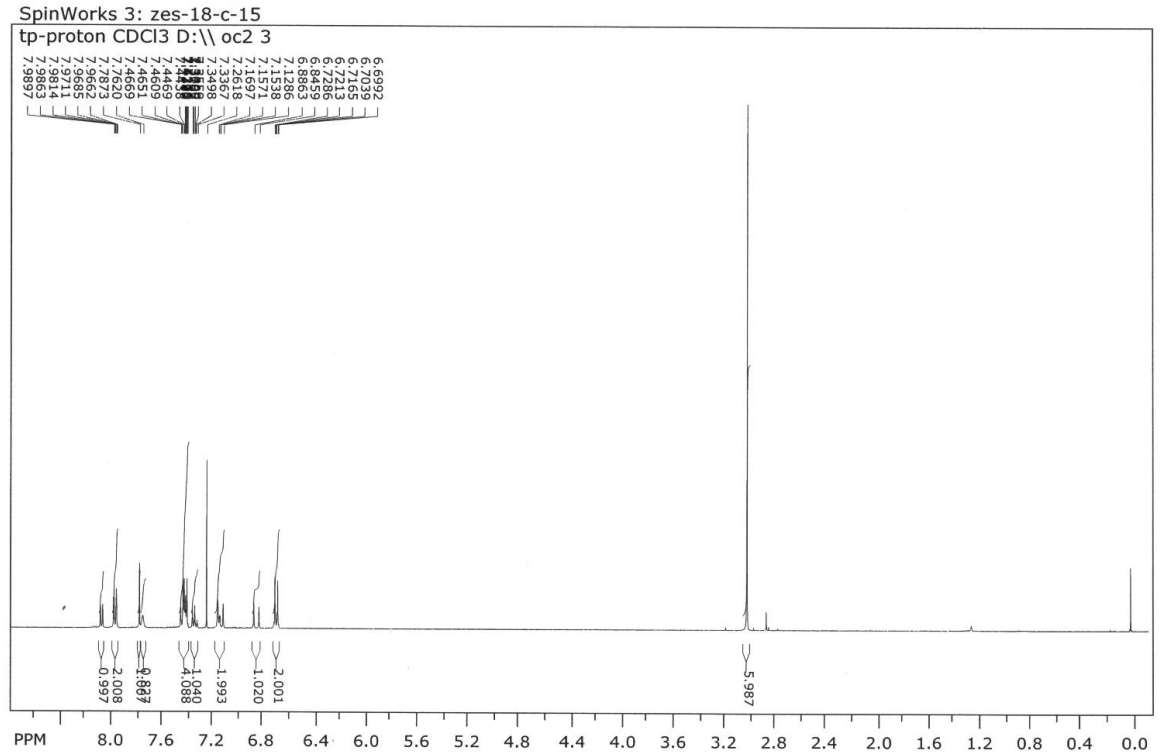

file: ...ers\Gast\Desktop\zes-18-c-15\1\fid expt: <zg45>
transmitter freq.: 400.133201 MHz
time domain size: 65536 points
width: 9578.54 Hz = 23.9384 ppm = 0.146157 Hz/pt
number of scans: 32

freq. of 0 ppm: 400.130009 MHz
processed size: 32768 complex points
LB: 0.000 GF: 0.0000
Hz/cm: 143.124 ppm/cm: 0.35769

Mass Spectrum of 5g

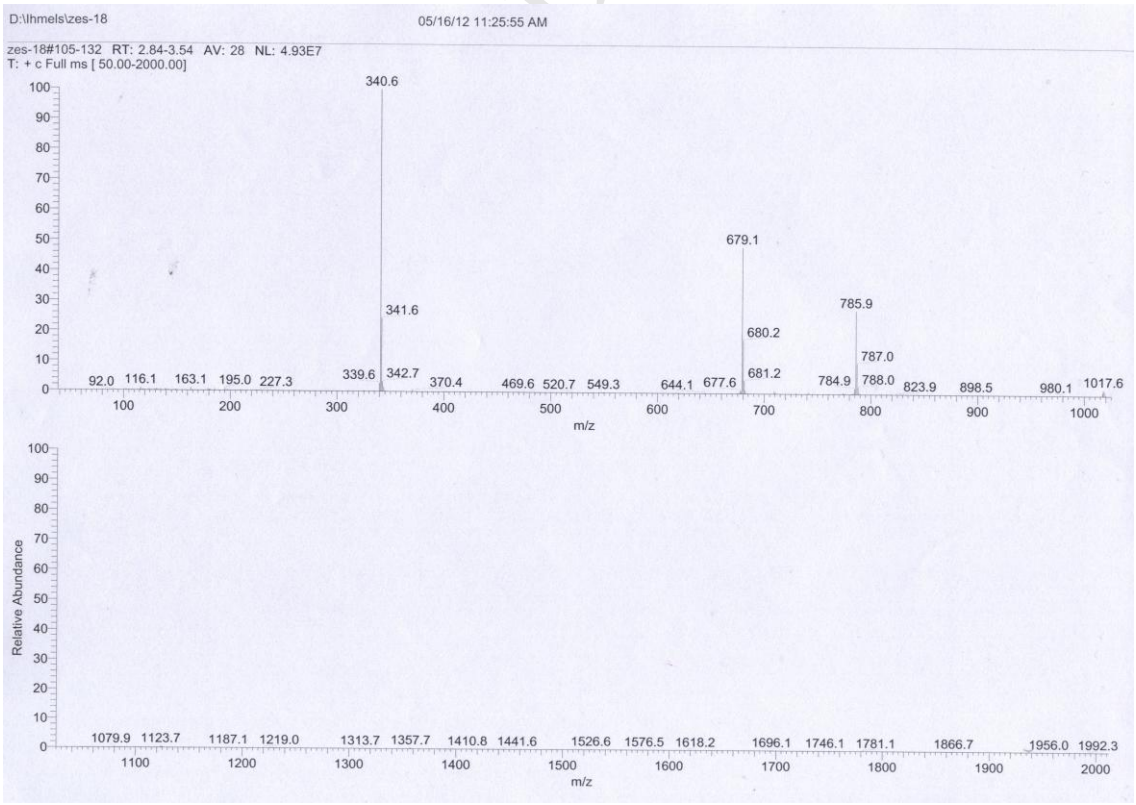

^{1}H-NMR Spectrum of 5h

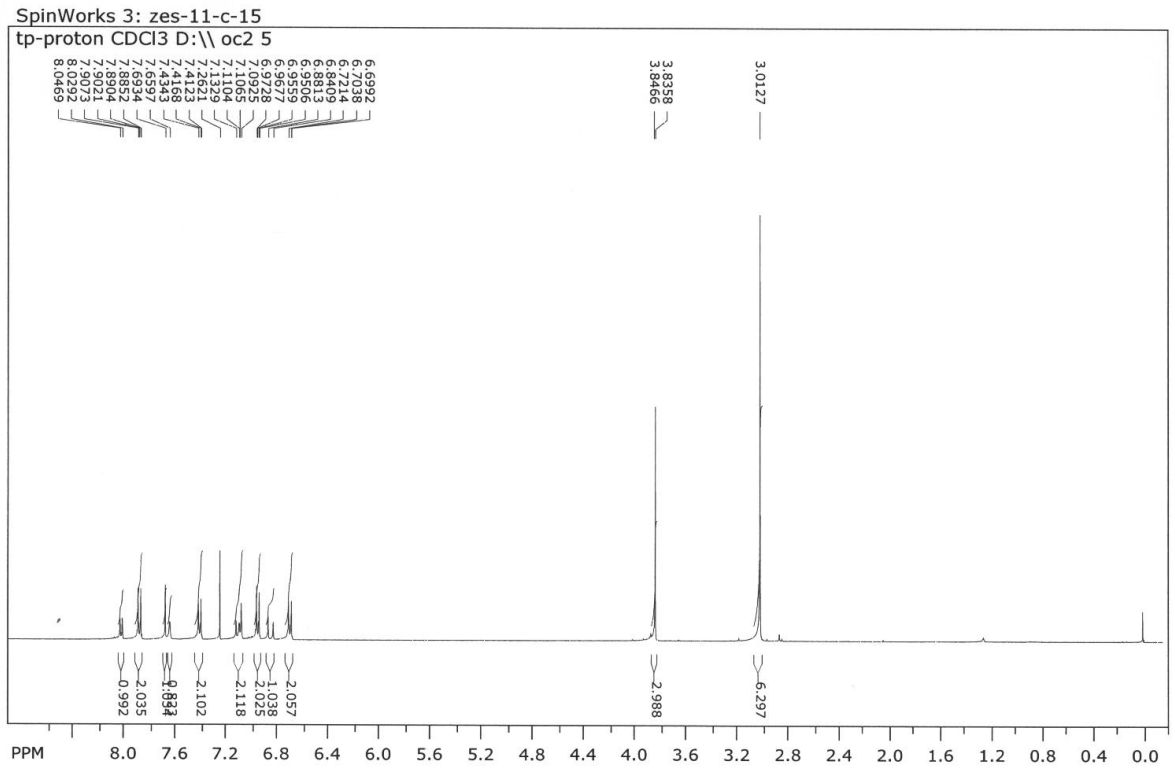

file: ...ers\Gast\Desktop\zes-11-c-15\1\fid expt: <zg45>
transmitter freq.: 400.133201 MHz
time domain size: 65536 points
width: 9578.54 Hz = 23.9384 ppm = 0.146157 Hz/pt
number of scans: 32

freq. of 0 ppm: 400.130009 MHz
processed size: 32768 complex points
LB: 0.000 GF: 0.0000
Hz/cm: 145.657 ppm/cm: 0.36402

Mass Spectrum of 5h

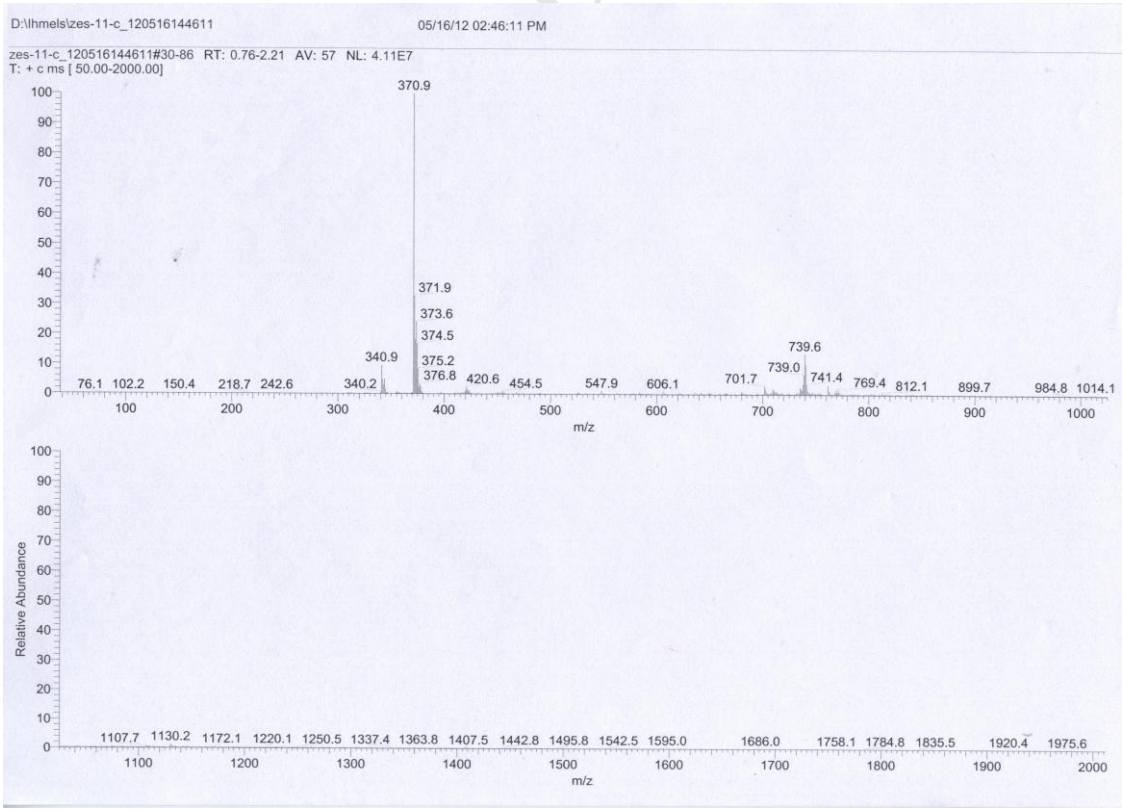

^{1}H-NMR Spectrum of 5i

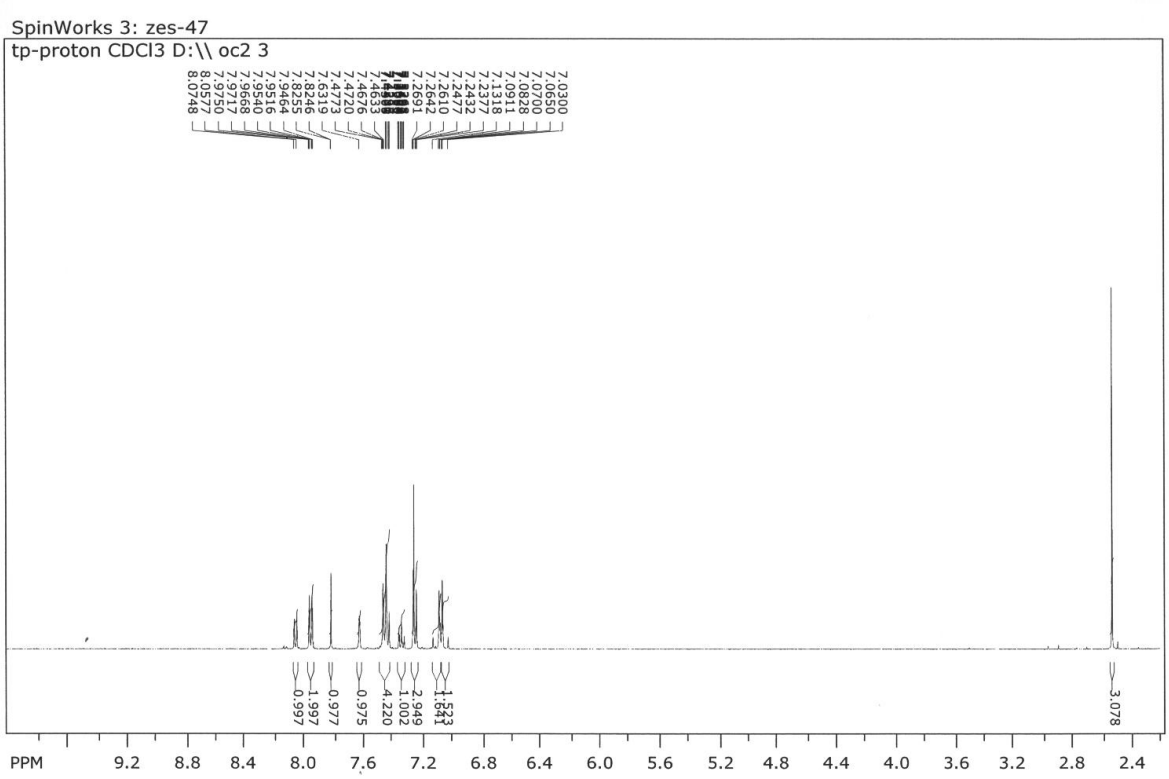

file: ...sers\Gast\Desktop\zes\zes-47\1\fid expt: <zg45>
transmitter freq.: 400.133201 MHz
time domain size: 65536 points
width: 9578.54 Hz = 23.9384 ppm = 0.146157 Hz/pt
number of scans: 32

freq. of 0 ppm: 400.130009 MHz
processed size: 32768 complex points
LB: 0.000 GF: 0.0000
Hz/cm: 125.392 ppm/cm: 0.31338

Mass Spectrum of 5i

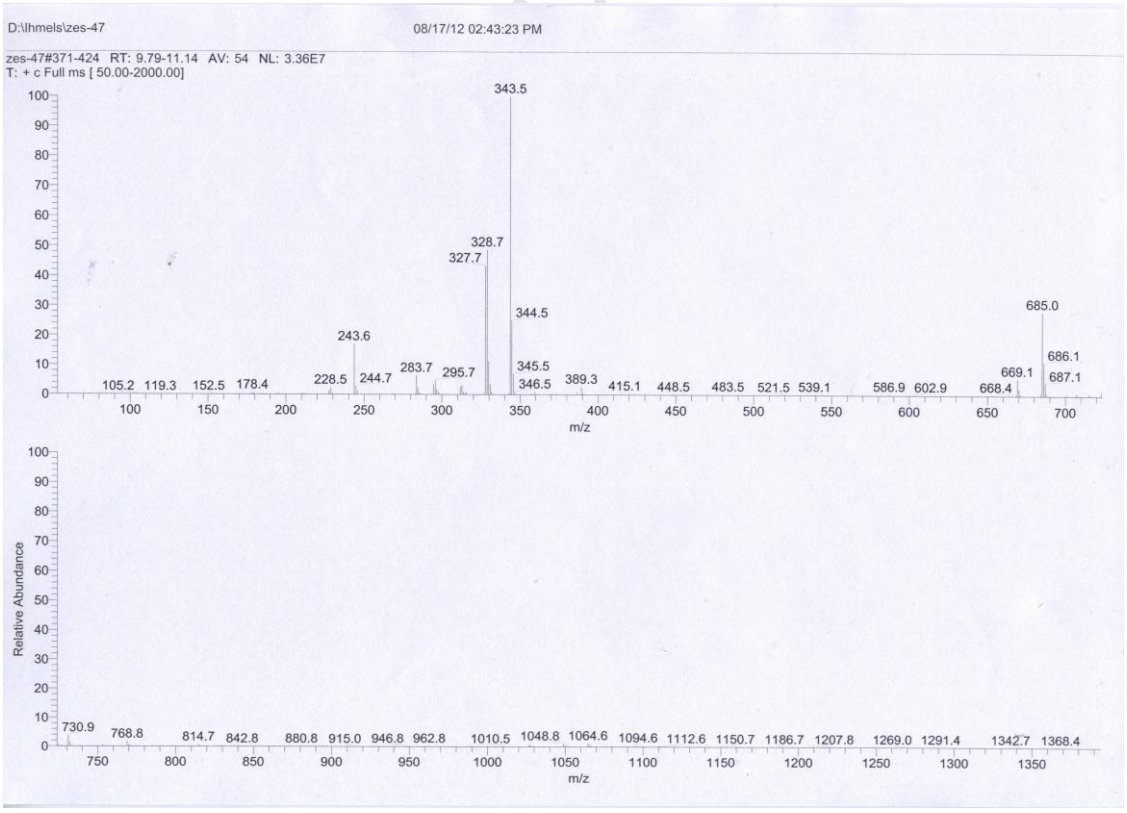

^{1}H-NMR Spectrum of 5j

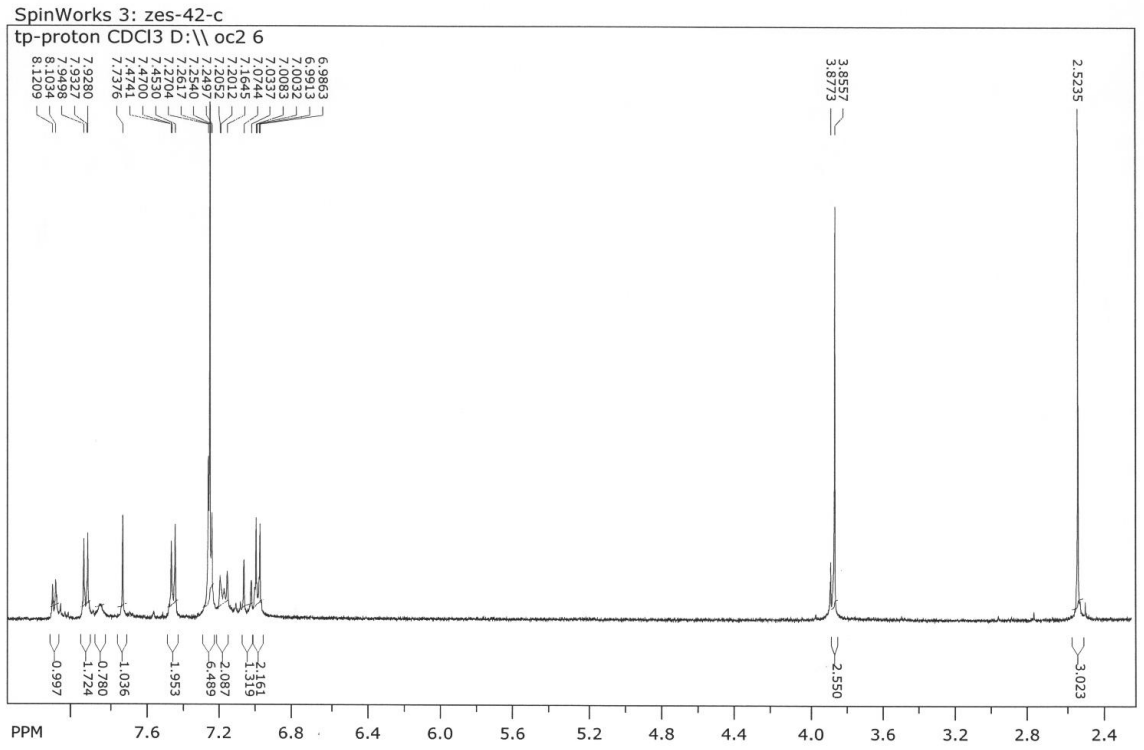

Mass Spectrum of 5j

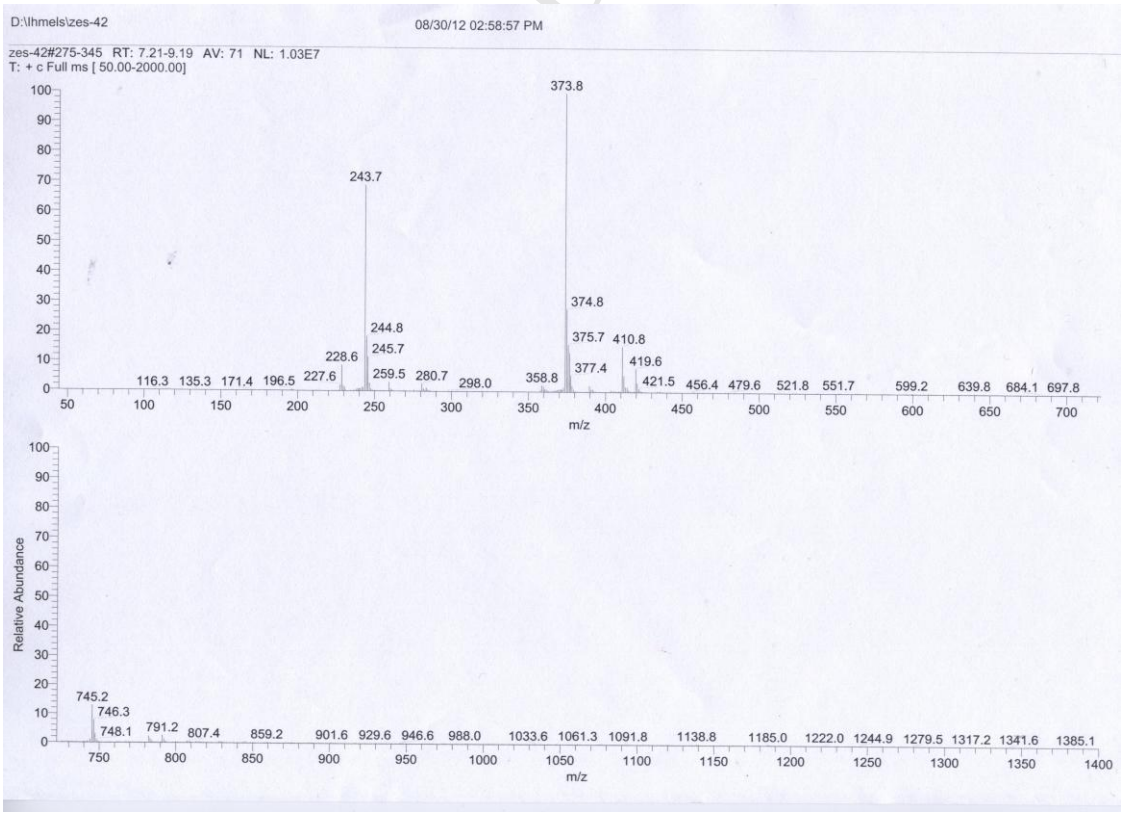

^{1}H-NMR Spectrum of 5k

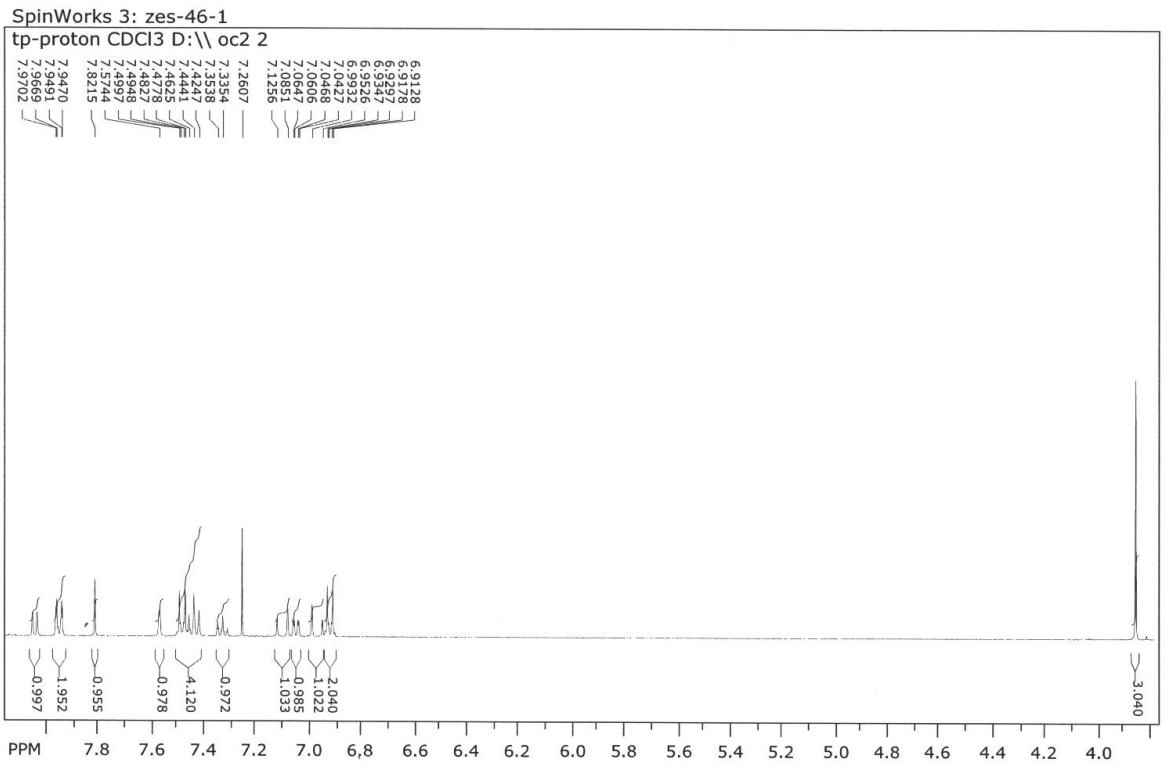

file: ...st\Desktop\zes\zes-46-1-C-13\1\fid expt: <zg45>
transmitter freq.: 400.133201 MHz
time domain size: 65536 points
width: 9578.54 Hz = 23.9384 ppm = 0.146157 Hz/pt
number of scans: 32

freq. of 0 ppm: 400.130009 MHz
processed size: 32768 complex points
LB: 0.000 GF: 0.0000
Hz/cm: 70.277 ppm/cm: 0.17563

Mass Spectrum of 5k

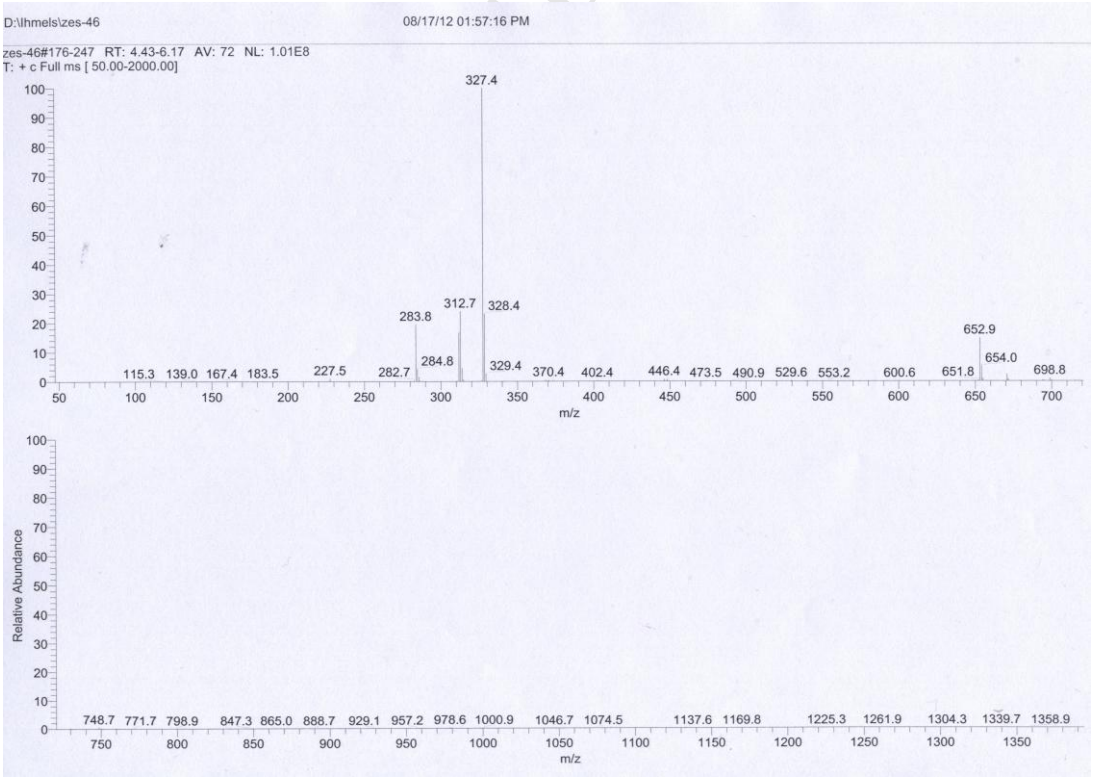

^{1}H-NMR Spectrum of 5l

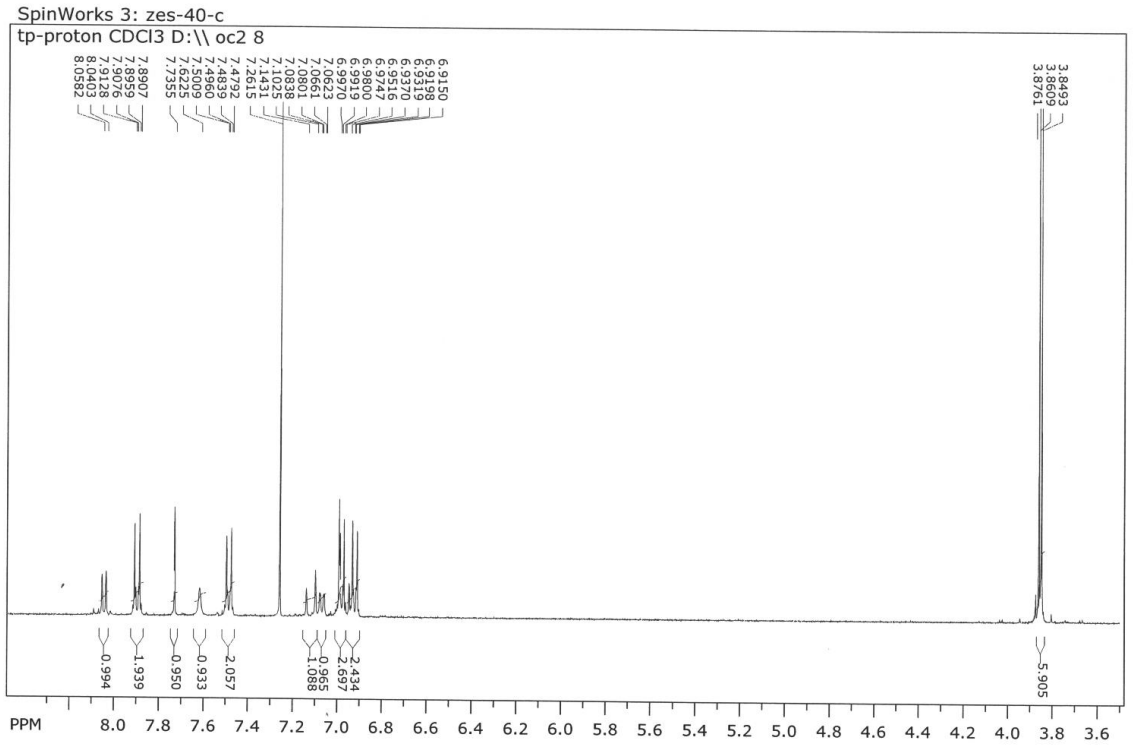

file: ...rs\Gast\Desktop\zes\zes-40-c\1\fid expt: <zg45>
transmitter freq.: 400.133201 MHz
time domain size: 65536 points
width: 9578.54 Hz = 23.9384 ppm = 0.146157 Hz/pt
number of scans: 32

freq. of 0 ppm: 400.130009 MHz
processed size: 32768 complex points
LB: 0.000 GF: 0.0000
Hz/cm: 79.795 ppm/cm: 0.19942

Mass Spectrum of 5l

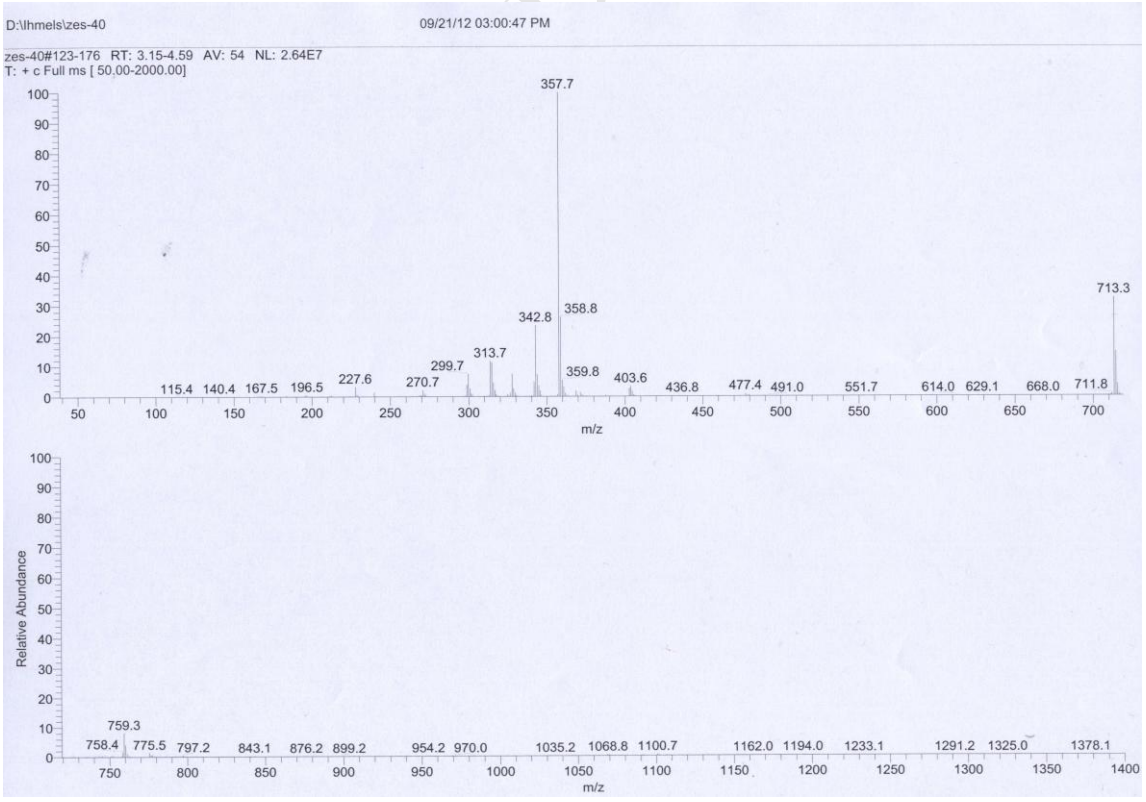

^{1}H-NMR Spectrum of 5m

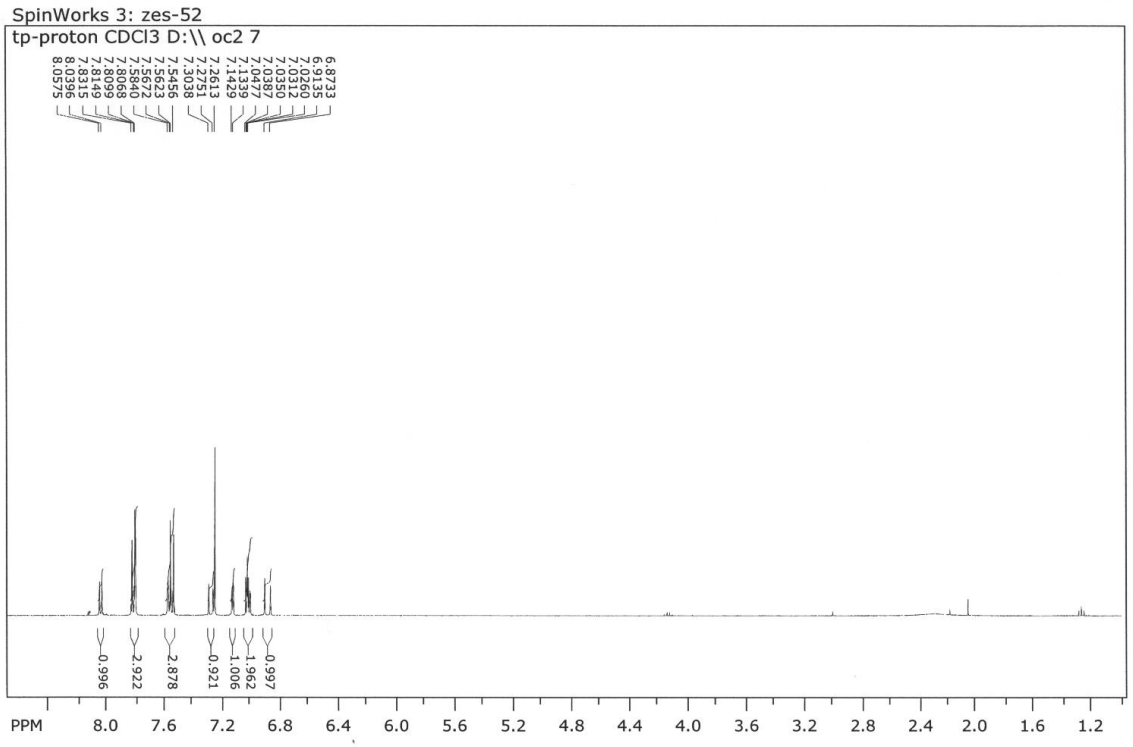

file: ...eport-first\neutral\zes-52-c\1\fid expt: <zg45>
transmitter freq.: 400.133201 MHz
time domain size: 65536 points
width: 9578.54 Hz = 23.9384 ppm = 0.146157 Hz/pt
number of scans: 32

freq. of 0 ppm: 400.130009 MHz
processed size: 32768 complex points
LB: 0.000 GF: 0.0000
Hz/cm: 123.492 ppm/cm: 0.30863

Mass Spectrum of 5m

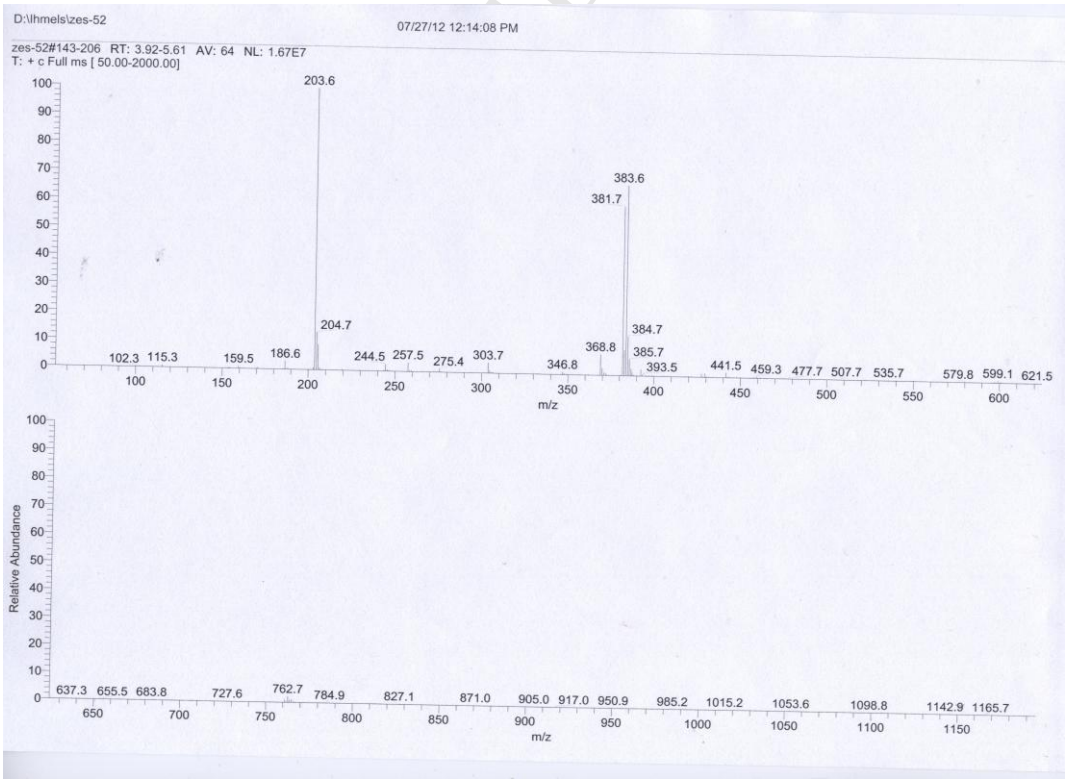

^{1}H-NMR Spectrum of 5n

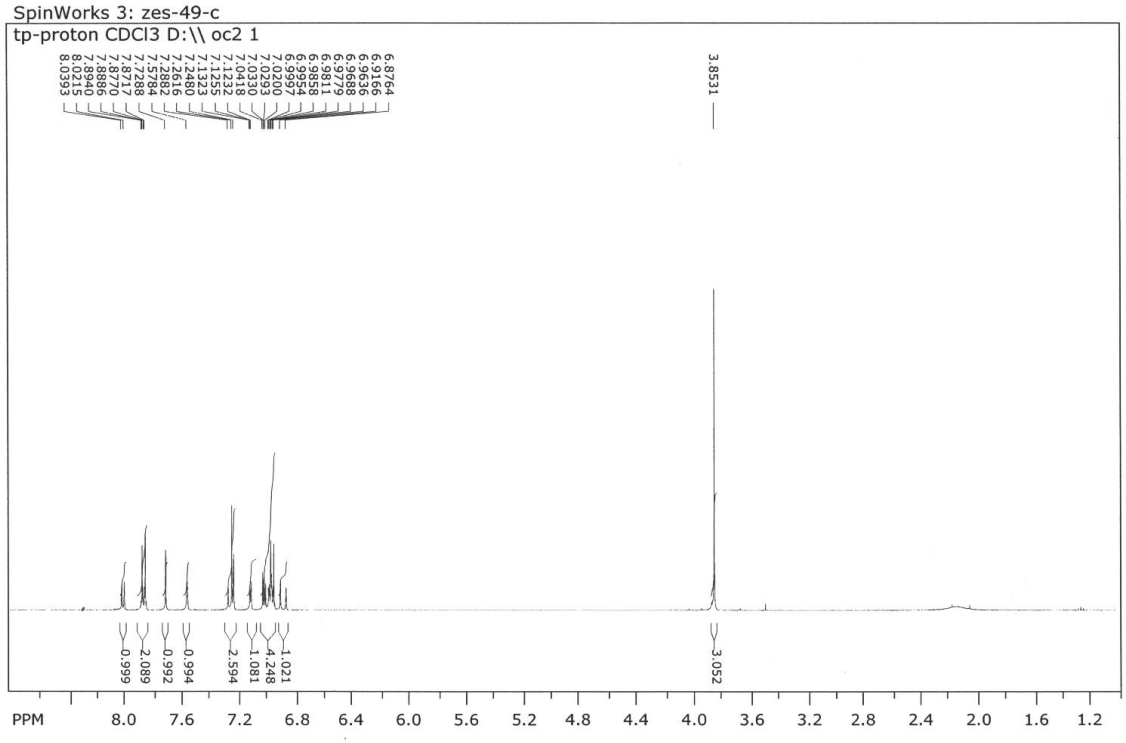

file: ...eport-first\neutral\zes-49-c\1\fid expt: <zg45>
transmitter freq.: 400.133201 MHz
time domain size: 65536 points
width: 9578.54 Hz = 23.9384 ppm = 0.146157 Hz/pt
number of scans: 32

freq. of 0 ppm: 400.130009 MHz
processed size: 32768 complex points
LB: 0.000 GF: 0.0000
Hz/cm: 125.392 ppm/cm: 0.31338

Mass Spectrum of 5n

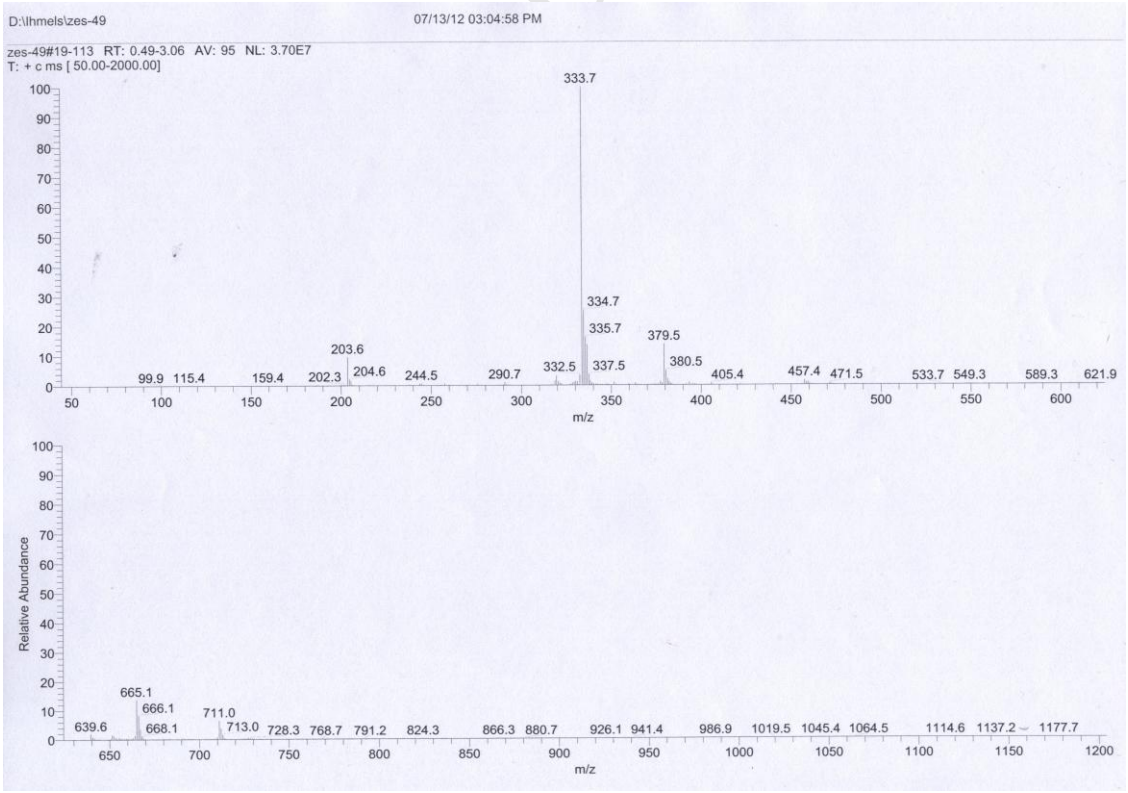

References

1. Demas, J.N.; Crosby, G.A. *J. Phys. Chem.* **1971**, *75*, 991-1024.
2. B. Valeur, *Molecular Fluorescence*, Wiley-VCH Verlag GmbH, Weinheim, 2002.